Cyclosporin A and its derivatives, which target cyclophilins, were shown to impair HCV RNA replication and to exhibit efficacy in hepatitis C patients (Watashi et al., 2003; Ishii et al., 2006). Inoue et al. (2003) reported cyclosporin A treatment of HCV in a clinical trial. Cyclosporin derivatives lacking the ability to interact with cyclophilin lost their inhibitory effect on HCV replication (Watashi et al., 2005). Cyclophilin B is reported to be a 20-kDa secreted neurotropic factor for spinal cord cells in chick embryos (Spik et al., 1991), and is secreted into human milk and blood (Spik et al., 1991; Allain et al., 1994). Cyclophilin B specifically interacts with NS5B, the HCV RNA-dependent RNA polymerase around the ER of the HCV replicon cells, and promotes NS5B's association with viral RNA (Watashi et al., 2005). Cyclosporin A (CsA) was shown to disrupt the interaction between NS5B and cyclophilin B (Watashi et al., 2005). Treatment with cyclosporin A and knockdown of cyclophilin B suppressed the replication of HCV. However, several groups reported that interaction between NS5A and cyclophilin A is more important for HCV replication than interaction between NS5B and cyclophilin B. There is a growing consensus that cyclophilin A in particular is a crucial factor during HCV replication. A number of point mutations in both NS5A and NS5B have been reported to be associated with *in vitro* resistance to cyclophilin A (Yang et al., 2008; Chatterji et al., 2009; Kaul et al., 2009). Direct interaction between cyclophilin A and NS5B or NS5A has been observed (Yang et al., 2008). Several CsA-analogs, i.e., NIM811 (Ma et al., 2006), DEB025, and SCY-635 (Hopkins et al., 2010), are currently in preclinical and clinical development. DEB025 disrupts the interaction between NS5A and cyclophilin A and suppresses cyclophilin A isomerase activity. Although experimental differences in cell lines and replicons may affect employment of cyclophilins in HCV replication, the main molecule targeted by the cyclosporin analogs used clinically so far seems to be cyclophilin A.

The treatment with CsA has been associated with increased susceptibility to atherosclerosis and the development of hyperlipidemia (reviewed by Kockx et al., 2010). Treatment with CsA upregulated activity of cholesteryl ester transfer protein and suppressed lipoprotein lipase activity (Tory et al., 2008). Upregulation of cholesteryl ester by cholesteryl ester transfer protein could lead to accumulation of lipoprotein with cholesteryl ester. The report by Anderson et al. (2011) suggests that cyclophilin A and cyclophilin 40 are important for not only viral replication, but also the release of infectious viral particles. NIM811 treatment suppresses virus production and viral RNA replication (Goto et al., 2006). NIM811 treatment led to enlargement of lipid droplets and apoB crescent formation in replicon cells, but not naïve Huh7 cell line, while decreasing apoB secretion and the number of lipid droplets, rendering NS5A dislocation with apoB (Anderson et al., 2011). Knockdown of cyclophilins A and 40 in replicon cells showed the similar changes in lipid droplets size and apoB localization, comparing with NIM811 treatment (Anderson et al., 2011). Cyclophilins A and 40 may regulate lipid trafficking in the presence of HCV proteins to support secretion of viral particles.

NS5A/B AND MEMBRANE-ASSOCIATED PROTEINS

Host lipids are well known to be essential components in the viral life cycle, including the assembly, budding, and replication of various viruses (Chen et al., 2005; Giese et al., 2006; Mannova et al., 2006; Oomens et al., 2006). In the case of HCV, several types of lipids are required for the HCV life cycle. Saturated and monounsaturated fatty acids, but not polyunsaturated fatty acids, enhance HCV RNA replication (Kapadia and Chisari, 2005), suggesting that lipid biogenesis is involved in HCV replication. HCV particles bind to lipoprotein receptors for entry (Agnello et al., 1999; Scarselli et al., 2002) and are believed to exist with lipoproteins in the serum of infected patients (Thomssen et al., 1992). There is also evidence that HCV uses the VLDL assembly and secretion pathway for maturation and secretion of viral particles (Huang et al., 2007; Gastaminza et al., 2008). Cholesterol and sphingolipids are employed for virion maturation and infectivity, since depletion of cholesterol or down-regulation of sphingomyelin reduces infectivity (Aizaki et al., 2008). Accumulation of lipid components in the liver leads to liver steatosis, and is associated with progression to liver fibrosis and hepatocellular carcinoma, as described above.

Hepatitis C virus replication is suppressed by an inhibitor of geranylgeranyl transferase I, but not by that of farnesyl transferase (Ye et al., 2003). Geranylgeranylate is known as an intermediate found in the mevalonate pathway and is covalently bound to various cellular proteins that are associated with plasma or the intracellular membrane (Horton et al., 2002). Immunoprecipitation analysis revealed that NS5A interacts with FBL2 (Wang et al., 2005a). The F-box motif is located in the N-terminus of FBL2, followed by 11 leucine-rich repeats (Ilyin et al., 1999) and the CAAX motif, which is thought to be modified by geranylgeranylation (Wang et al., 2005a). The F-box motif is generally essential for the formation of the ubiquitin ligase complex (Ilyin et al., 1999), suggesting that FBL2 regulates the ubiquitination of host or viral proteins through the interaction with NS5A. Another possibility is that FBL2 retains the viral replication complex by interacting with NS5A (**Figure 3**, step 3).

Screening of a genome-wide siRNA library revealed phosphatidylinositol 4-kinase III alpha (PI4KA) and COPI vesicle coat complex as a human gene associated with HCV replication (Bigger et al., 2004; Borawski et al., 2009; Li et al., 2009; Tai et al., 2009; Trotard et al., 2009; Vaillancourt et al., 2009; Reiss et al., 2011). Phosphatidylinositol 4-phosphate, which is associated with oxysterol binding protein (OSBP) and CERT (Peretti et al., 2008; Banerji et al., 2010) as described below, is increased by HCV infection (Bigger et al., 2004; Hsu et al., 2010; Reiss et al., 2011; Tai and Salloum, 2011). PI4KA is co-localized with NS5A and double stranded RNA in the replication platform composed of detergent-resistant lipid components, known as a membranous web, and is critical for HCV replication at posttranslational stages in the membranous web (Berger et al., 2009). NS5A can interact with PI4KA (Berger et al., 2011; Lim and Hwang, 2011; Reiss et al., 2011) and recruit PI4KA to the membranous web (Berger et al., 2009; Tai et al., 2009; Reiss et al., 2011; Tai and Salloum, 2011). Furthermore, PI4KA, but not phosphatidylinositol 4-kinase III beta, induces the membranous web structure under the non-replicative condition (Berger et al., 2011; Lim and Hwang, 2011; Reiss et al., 2011). Biosynthesis of phosphatidylinositol 4-phosphate by PI4KA that is recruited by NS5A in the membranous web may be required for HCV replication and can be an endogenous biomarker of the membranous web (**Figure 3**, step 3).

Vesicle-associated membrane protein-associated proteins were originally identified as proteins that bind to vesicle-associated membrane protein (VAMP) in the nematode *Aplysia* and were designated as VAMP-associated protein 33 kDa (later renamed VAP-A; Skehel et al., 1995). Furthermore, one homolog and its splicing variant were reported as VAP-B and -C, respectively (Nishimura et al., 1999). VAP is classified as a type II membrane protein, and is composed of three functional domains: major sperm protein (MSP), which occupies the N-terminal half region, the coiled-coil domain, and the transmembrane domain. VAP-A shares 60% identity with VAP-B, while VAP-C is the splicing variant of VAP-B that lacks the coiled-coil and transmembrane domains (Nishimura et al., 1999). GST pull-down and immunoprecipitation analyses revealed that NS5A and NS5B interact with human VAP-A/B and that the N-terminal MSP domain and the coiled-coil domain of VAP-A/B are responsible for the binding to NS5B and NS5A, respectively (Tu et al., 1999; Hamamoto et al., 2005). In addition, systematic RNAi screening revealed that 62 target host genes are involved in HCV RNA or proteins including VAP-A/B (Randall et al., 2007). Several reports suggest that HCV replication takes place on the membranous web (Shi et al., 2003; Gao et al., 2004; Sakamoto et al., 2005). NS4B is predominantly associated with a lipid-raft-like detergent-resistant fraction equivalent to the membranous web, and both NS5A and NS5B were co-localized in a similar fraction in the presence of NS4B (Sakamoto et al., 2005). VAP-A was also localized in a detergent-resistant fraction, suggesting that it plays an important role in HCV replication because the dominant negative mutant of VAP-A suppressed the replication of HCV RNA (Gao et al., 2004). VAP-B forms a homodimer and heterodimer with VAP-A, and knockdown of VAP-A or VAP-B led to substantial suppression of HCV replication (Hamamoto et al., 2005). These findings suggest that VAP-A and -B positively regulate HCV replication by binding to NS5A/B.

The physiological function of VAPs was reported to be trafficking of ceramide and cholesterol between ER and the Golgi apparatus. Several VAP-interacting proteins share the FFAT motif (two phenylalanines in an acidic tract), which has the consensus amino acid sequence EFFDAxE, as determined by a comparison among oxysterol binding proteins, OSBP-related proteins (ORPs; Loewen et al., 2003), and the ceramide transport protein CERT (Hanada et al., 2003; Kawano et al., 2006), contributing to the regulation of lipid metabolism. OSBP binds and transports cholesterol or hydroxycholesterol from ER to the Golgi (Ridgway et al., 1992; Wang et al., 2005b), while CERT binds and transports ceramide from ER to the Golgi, where the ceramide is converted to sphingolipids (Kumagai et al., 2005). Altering the sphingomyelin/ceramide ratio of the plasma membrane can effect HCV entry via the cell surface expression of CD81 (Voisset et al., 2008). OSBP mediates HCV secretion while binding to NS5A and VAP-A (Amako et al., 2009). Inhibition of CERT function effectively suppressed HCV release regardless of RNA replication (Aizaki et al., 2008). Phosphorylation of CERT and OSBP by protein kinase D negatively regulates VAPs binding to CERT and OSBP resulting in an effect on HCV infection (Amako et al., 2011). HCV NS5A may allow VAP-A/B to provide ceramide and cholesterol to replication complexes for upregulation of virus propagation (**Figure 3**, step 3).

The VAP-B-splicing variant VAP-C interacts with NS5B via the short form of the MSP domain and then suppresses the HCV replication by disrupting binding of other VAPs to NS5B (Kukihara et al., 2009). Expression of VAP-C is observed in various tissues except for the liver, suggesting that tissue distribution of VAP-C determines the tropism of HCV infection (Kukihara et al., 2009). These findings suggest that VAP-C negatively regulates HCV replication by inhibiting the interaction between VAP-A/B and NS5B. Furthermore, expression of VAP-C was negligible in B cells prepared from chronic hepatitis C patients, in whom B cells included HCV particles (Ito et al., 2010), and expression of the full HCV genome in B cells induced B-cell lymphoma in a conditional transgenic mouse (Kasama et al., 2010), suggesting that HCV infection increases the chance of developing B-cell lymphomas via dysregulation of lipid metabolism.

CONCLUSION

This review summarizes several recently reported viral and host factors that exploit lipid components to support HCV infection. The mechanism by which HCV proteins cooperate with host factors to exploit lipid components and to regulate lipid metabolism in the infection has not been elucidated completely. The aim of identifying host factors is effective and stable therapy; targeting the host factors might be done to prevent the emergence of resistant viruses. Cyclosporin analogs will be used clinically in the near future. Wide screening and proteomics analyses have revealed novel host factors that are required for HCV replications over the past decade. The mechanism by which HCV infection induces formation of membranous web in infected cells has been unknown yet, although NS4B is involved in formation of membranous web (Egger et al., 2002; Gosert et al., 2005; Ferraris et al., 2010). We also found several host proteins to be NS4B-associating host factors by proteomics analysis based on the TargetMine program (Tripathi et al., 2010). Further study will be required to identify the prominent factors essential for lipid metabolism that are associated with each step in the HCV life cycle and to develop effective and stable therapies for hepatitis C.

ACKNOWLEDGMENTS

We thank R. Tanaka for her secretarial work. Our original work cited here were supported in part by grants-in-aid from the Ministry of Health, Labor, and Welfare (Research on Hepatitis); the Ministry of Education, Culture, Sports, Science, and Technology.

REFERENCES

Adinolfi, L. E., Gambardella, M., Andreana, A., Tripodi, M. F., Utili, R., and Ruggiero, G. (2001). Steatosis accelerates the progression of liver damage of chronic hepatitis C patients and correlates with specific HCV genotype and visceral obesity. *Hepatology* 33, 1358–1364.

Agnello, V., Abel, G., Elfahal, M., Knight, G. B., and Zhang, Q. X. (1999). Hepatitis C virus and other Flaviviridae viruses enter cells via low density lipoprotein receptor. *Proc. Natl. Acad. Sci. U.S.A.* 96, 12766–12771.

Aizaki, H., Lee, K. J., Sung, V. M., Ishiko, H., and Lai, M. M. (2004). Characterization of the hepatitis C virus RNA replication complex associated with lipid rafts. *Virology* 324, 450–461.

Aizaki, H., Morikawa, K., Fukasawa, M., Hara, H., Inoue, Y., Tani, H., Saito, K., Nishijima, M., Hanada, K., Matsuura, Y., Lai, M. M., Miyamura, T., Wakita, T., and Suzuki, T. (2008). Critical role of virion-associated cholesterol and sphingolipid in hepatitis C virus infection. *J. Virol.* 82, 5715–5724.

Albecka, A., Belouzard, S., De Beeck, A. O., Descamps, V., Goueslain, L., Bertrand-Michel, J., Terce, F., Duverlie, G., Rouille, Y., and Dubuisson, J. (2012). Role of LDL receptor in the hepatitis c virus life cycle. *Hepatology*. doi: 10.1002/hep.25501

Allain, F., Denys, A., and Spik, G. (1994). Characterization of surface binding sites for cyclophilin B on a human tumor T-cell line. *J. Biol. Chem.* 269, 16537–16540.

Amako, Y., Sarkeshik, A., Hotta, H., Yates, J. III, and Siddiqui, A. (2009). Role of oxysterol binding protein in hepatitis C virus infection. *J. Virol.* 83, 9237–9246.

Amako, Y., Syed, G. H., and Siddiqui, A. (2011). Protein kinase D negatively regulates hepatitis C virus secretion through phosphorylation of oxysterol-binding protein and ceramide transfer protein. *J. Biol. Chem.* 286, 11265–11274.

Anderson, L. J., Lin, K., Compton, T., and Wiedmann, B. (2011). Inhibition of cyclophilins alters lipid trafficking and blocks hepatitis C virus secretion. *Virol. J.* 8, 329.

Andre, P., Komurian-Pradel, F., Deforges, S., Perret, M., Berland, J. L., Sodoyer, M., Pol, S., Brechot, C., Paranhos-Baccala, G., and Lotteau, V. (2002). Characterization of low- and very-low-density hepatitis C virus RNA-containing particles. *J. Virol.* 76, 6919–6928.

Banerji, S., Ngo, M., Lane, C. F., Robinson, C. A., Minogue, S., and Ridgway, N. D. (2010). Oxysterol binding protein-dependent activation of sphingomyelin synthesis in the golgi apparatus requires phosphatidylinositol 4-kinase IIalpha. *Mol. Biol. Cell* 21, 4141–4150.

Barba, G., Harper, F., Harada, T., Kohara, M., Goulinet, S., Matsuura, Y., Eder, G., Schaff, Z., Chapman, M. J., Miyamura, T., and Brechot, C. (1997). Hepatitis C virus core protein shows a cytoplasmic localization and associates to cellular lipid storage droplets. *Proc. Natl. Acad. Sci. U.S.A.* 94, 1200–1205.

Barth, H., Schafer, C., Adah, M. I., Zhang, F., Linhardt, R. J., Toyoda, H., Kinoshita-Toyoda, A., Toida, T., Van Kuppevelt, T. H., Depla, E., Von Weizsacker, F., Blum, H. E., and Baumert, T. F. (2003). Cellular binding of hepatitis C virus envelope glycoprotein E2 requires cell surface heparan sulfate. *J. Biol. Chem.* 278, 41003–41012.

Bartosch, B., Vitelli, A., Granier, C., Goujon, C., Dubuisson, J., Pascale, S., Scarselli, E., Cortese, R., Nicosia, A., and Cosset, F. L. (2003). Cell entry of hepatitis C virus requires a set of co-receptors that include the CD81 tetraspanin and the SR-B1 scavenger receptor. *J. Biol. Chem.* 278, 41624–41630.

Benga, W. J., Krieger, S. E., Dimitrova, M., Zeisel, M. B., Parnot, M., Lupberger, J., Hildt, E., Luo, G., Mclauchlan, J., Baumert, T. F., and Schuster, C. (2010). Apolipoprotein E interacts with hepatitis C virus nonstructural protein 5A and determines assembly of infectious particles. *Hepatology* 51, 43–53.

Berger, K. L., Cooper, J. D., Heaton, N. S., Yoon, R., Oakland, T. E., Jordan, T. X., Mateu, G., Grakoui, A., and Randall, G. (2009). Roles for endocytic trafficking and phosphatidylinositol 4-kinase III alpha in hepatitis C virus replication. *Proc. Natl. Acad. Sci. U.S.A.* 106, 7577–7582.

Berger, K. L., Kelly, S. M., Jordan, T. X., Tartell, M. A., and Randall, G. (2011). Hepatitis C virus stimulates the phosphatidylinositol 4-kinase III alpha-dependent phosphatidylinositol 4-phosphate production that is essential for its replication. *J. Virol.* 85, 8870–8883.

Bigger, C. B., Guerra, B., Brasky, K. M., Hubbard, G., Beard, M. R., Luxon, B. A., Lemon, S. M., and Lanford, R. E. (2004). Intrahepatic gene expression during chronic hepatitis C virus infection in chimpanzees. *J. Virol.* 78, 13779–13792.

Blanchard, E., Belouzard, S., Goueslain, L., Wakita, T., Dubuisson, J., Wychowski, C., and Rouille, Y. (2006). Hepatitis C virus entry depends on clathrin-mediated endocytosis. *J. Virol.* 80, 6964–6972.

Blight, K. J., Kolykhalov, A. A., and Rice, C. M. (2000). Efficient initiation of HCV RNA replication in cell culture. *Science* 290, 1972–1974.

Boguszewska-Chachulska, A. M., Krawczyk, M., Stankiewicz, A., Gozdek, A., Haenni, A. L., and Strokovskaya, L. (2004). Direct fluorometric measurement of hepatitis C virus helicase activity. *FEBS Lett.* 567, 253–258.

Borawski, J., Troke, P., Puyang, X., Gibaja, V., Zhao, S., Mickanin, C., Leighton-Davies, J., Wilson, C. J., Myer, V., Cornellataracido, I., Baryza, J., Tallarico, J., Joberty, G., Bantscheff, M., Schirle, M., Bouwmeester, T., Mathy, J. E., Lin, K., Compton, T., Labow, M., Wiedmann, B., and Gaither, L. A. (2009). Class III phosphatidylinositol 4-kinase alpha and beta are novel host factor regulators of hepatitis C virus replication. *J. Virol.* 83, 10058–10074.

Borowski, P., Deinert, J., Schalinski, S., Bretner, M., Ginalski, K., Kulikowski, T., and Shugar, D. (2003). Halogenated benzimidazoles and benzotriazoles as inhibitors of the NTPase/helicase activities of hepatitis C and related viruses. *Eur. J. Biochem.* 270, 1645–1653.

Boson, B., Granio, O., Bartenschlager, R., and Cosset, F. L. (2011). A concerted action of hepatitis C virus p7 and nonstructural protein 2 regulates core localization at the endoplasmic reticulum and virus assembly. *PLoS Pathog.* 7, e1002144. doi:10.1371/journal.ppat.1002144

Bradley, D., Mccaustland, K., Krawczynski, K., Spelbring, J., Humphrey, C., and Cook, E. H. (1991). Hepatitis C virus: buoyant density of the factor VIII-derived isolate in sucrose. *J. Med. Virol.* 34, 206–208.

Brodsky, J. L., Gusarova, V., and Fisher, E. A. (2004). Vesicular trafficking of hepatic apolipoprotein B100 and its maturation to very low-density lipoprotein particles; studies from cells and cell-free systems. *Trends Cardiovasc. Med.* 14, 127–132.

Carabaich, A., Ruvoletto, M., Bernardinello, E., Tono, N., Cavalletto, L., Chemello, L., Gatta, A., and Pontisso, P. (2005). Profiles of HCV core protein and viremia in chronic hepatitis C: possible protective role of core antigen in liver damage. *J. Med. Virol.* 76, 55–60.

Carrere-Kremer, S., Montpellier-Pala, C., Cocquerel, L., Wychowski, C., Penin, F., and Dubuisson, J. (2002). Subcellular localization and topology of the p7 polypeptide of hepatitis C virus. *J. Virol.* 76, 3720–3730.

Cerutti, A., Maillard, P., Minisini, R., Vidalain, P. O., Roohvand, F., Pecheur, E. I., Pirisi, M., and Budkowska, A. (2011). Identification of a functional, CRM-1-dependent nuclear export signal in hepatitis C virus core protein. *PLoS ONE* 6, e25854. doi:10.1371/journal.pone.0025854

Chang, K. S., Jiang, J., Cai, Z., and Luo, G. (2007). Human apolipoprotein E is required for infectivity and production of hepatitis C virus in cell culture. *J. Virol.* 81, 13783–13793.

Chatel-Chaix, L., Melancon, P., Racine, M. E., Baril, M., and Lamarre, D. (2011). Y-box-binding protein 1 interacts with hepatitis C virus NS3/4A and influences the equilibrium between viral RNA replication and infectious particle production. *J. Virol.* 85, 11022–11037.

Chatterji, U., Bobardt, M., Selvarajah, S., Yang, F., Tang, H., Sakamoto, N., Vuagniaux, G., Parkinson, T., and Gallay, P. (2009). The isomerase active site of cyclophilin A is critical for hepatitis C virus replication. *J. Biol. Chem.* 284, 16998–17005.

Chen, B. J., Takeda, M., and Lamb, R. A. (2005). Influenza virus hemagglutinin (H3 subtype) requires palmitoylation of its cytoplasmic tail for assembly: M1 proteins of two subtypes differ in their ability to support assembly. *J. Virol.* 79, 13673–13684.

Chen, X., Barton, L. F., Chi, Y., Clurman, B. E., and Roberts, J. M. (2007). Ubiquitin-independent degradation of cell-cycle inhibitors by the REGgamma proteasome. *Mol. Cell* 26, 843–852.

Cheng, G., Zhong, J., and Chisari, F. V. (2006). Inhibition of dsRNA-induced signaling in hepatitis C virus-infected cells by NS3 protease-dependent and -independent mechanisms. *Proc. Natl. Acad. Sci. U.S.A.* 103, 8499–8504.

Codran, A., Royer, C., Jaeck, D., Bastien-Valle, M., Baumert, T. F., Kieny, M. P., Pereira, C. A., and Martin, J. P. (2006). Entry of hepatitis C virus pseudotypes into primary human hepatocytes by clathrin-dependent endocytosis. *J. Gen. Virol.* 87, 2583–2593.

Counihan, N. A., Rawlinson, S. M., and Lindenbach, B. D. (2011). Trafficking of hepatitis C virus core protein during virus particle assembly. *PLoS Pathog.* 7, e1002302. doi:10.1371/journal.ppat.1002302

Cun, W., Jiang, J., and Luo, G. (2010). The C-terminal alpha-helix domain of apolipoprotein E is required for interaction with nonstructural protein 5A and assembly of hepatitis C virus. *J. Virol.* 84, 11532–11541.

De Francesco, R., Tomei, L., Altamura, S., Summa, V., and Migliaccio, G. (2003). Approaching a new era for hepatitis C virus therapy: inhibitors of the NS3-4A serine protease and the NS5B RNA-dependent RNA polymerase. *Antiviral Res.* 58, 1–16.

Dentzer, T. G., Lorenz, I. C., Evans, M. J., and Rice, C. M. (2009). Determinants of the hepatitis C virus nonstructural protein 2 protease domain required for production of infectious virus. *J. Virol.* 83, 12702–12713.

Dhanak, D., Duffy, K. J., Johnston, V. K., Lin-Goerke, J., Darcy, M., Shaw, A. N., Gu, B., Silverman, C., Gates, A. T., Nonnemacher, M. R., Earnshaw, D. L., Casper, D. J., Kaura, A., Baker, A., Greenwood, C., Gutshall, L. L., Maley, D., Delvecchio, A., Macarron, R., Hofmann, G. A., Alnoah, Z., Cheng, H. Y., Chan, G., Khandekar, S., Keenan, R. M., and Sarisky, R.

T. (2002). Identification and biological characterization of heterocyclic inhibitors of the hepatitis C virus RNA-dependent RNA polymerase. *J. Biol. Chem.* 277, 38322–38327.

Egger, D., Wolk, B., Gosert, R., Bianchi, L., Blum, H. E., Moradpour, D., and Bienz, K. (2002). Expression of hepatitis C virus proteins induces distinct membrane alterations including a candidate viral replication complex. *J. Virol.* 76, 5974–5984.

Evans, M. J., Von Hahn, T., Tscherne, D. M., Syder, A. J., Panis, M., Wolk, B., Hatziioannou, T., Mckeating, J. A., Bieniasz, P. D., and Rice, C. M. (2007). Claudin-1 is a hepatitis C virus co-receptor required for a late step in entry. *Nature* 446, 801–805.

Failla, C., Tomei, L., and De Francesco, R. (1994). Both NS3 and NS4A are required for proteolytic processing of hepatitis C virus nonstructural proteins. *J. Virol.* 68, 3753–3760.

Failla, C., Tomei, L., and De Francesco, R. (1995). An amino-terminal domain of the hepatitis C virus NS3 protease is essential for interaction with NS4A. *J. Virol.* 69, 1769–1777.

Ferraris, P., Blanchard, E., and Roingeard, P. (2010). Ultrastructural and biochemical analyses of hepatitis C virus-associated host cell membranes. *J. Gen. Virol.* 91, 2230–2237.

Ferreon, J. C., Ferreon, A. C., Li, K., and Lemon, S. M. (2005). Molecular determinants of TRIF proteolysis mediated by the hepatitis C virus NS3/4A protease. *J. Biol. Chem.* 280, 20483–20492.

Fischer, G., Wittmann-Liebold, B., Lang, K., Kiefhaber, T., and Schmid, F. X. (1989). Cyclophilin and peptidyl-prolyl cis-trans isomerase are probably identical proteins. *Nature* 337, 476–478.

Foy, E., Li, K., Sumpter, R. Jr., Loo, Y. M., Johnson, C. L., Wang, C., Fish, P. M., Yoneyama, M., Fujita, T., Lemon, S. M., and Gale, M. Jr. (2005). Control of antiviral defenses through hepatitis C virus disruption of retinoic acid-inducible gene-I signaling. *Proc. Natl. Acad. Sci. U.S.A.* 102, 2986–2991.

Gao, L., Aizaki, H., He, J. W., and Lai, M. M. (2004). Interactions between viral nonstructural proteins and host protein hVAP-33 mediate the formation of hepatitis C virus RNA replication complex on lipid raft. *J. Virol.* 78, 3480–3488.

Gastaminza, P., Cheng, G., Wieland, S., Zhong, J., Liao, W., and Chisari, F. V. (2008). Cellular determinants of hepatitis C virus assembly, maturation, degradation, and secretion. *J. Virol.* 82, 2120–2129.

Giese, S. I., Woerz, I., Homann, S., Tibroni, N., Geyer, M., and Fackler, O. T. (2006). Specific and distinct determinants mediate membrane binding and lipid raft incorporation of HIV-1(SF2) Nef. *Virology* 355, 175–191.

Gosert, R., Jendrsczok, W., Berke, J. M., Brass, V., Blum, H. E., and Moradpour, D. (2005). Characterization of nonstructural protein membrane anchor deletion mutants expressed in the context of the hepatitis C virus polyprotein. *J. Virol.* 79, 7911–7917.

Goto, K., Watashi, K., Murata, T., Hishiki, T., Hijikata, M., and Shimotohno, K. (2006). Evaluation of the anti-hepatitis C virus effects of cyclophilin inhibitors, cyclosporin A, and NIM811. *Biochem. Biophys. Res. Commun.* 343, 879–884.

Grakoui, A., Mccourt, D. W., Wychowski, C., Feinstone, S. M., and Rice, C. M. (1993a). Characterization of the hepatitis C virus-encoded serine proteinase: determination of proteinase-dependent polyprotein cleavage sites. *J. Virol.* 67, 2832–2843.

Grakoui, A., Mccourt, D. W., Wychowski, C., Feinstone, S. M., and Rice, C. M. (1993b). A second hepatitis C virus-encoded proteinase. *Proc. Natl. Acad. Sci. U.S.A.* 90, 10583–10587.

Grakoui, A., Wychowski, C., Lin, C., Feinstone, S. M., and Rice, C. M. (1993c). Expression and identification of hepatitis C virus polyprotein cleavage products. *J. Virol.* 67, 1385–1395.

Hamamoto, I., Nishimura, Y., Okamoto, T., Aizaki, H., Liu, M., Mori, Y., Abe, T., Suzuki, T., Lai, M. M., Miyamura, T., Moriishi, K., and Matsuura, Y. (2005). Human VAP-B is involved in hepatitis C virus replication through interaction with NS5A and NS5B. *J. Virol.* 79, 13473–13482.

Hanada, K., Kumagai, K., Yasuda, S., Miura, Y., Kawano, M., Fukasawa, M., and Nishijima, M. (2003). Molecular machinery for non-vesicular trafficking of ceramide. *Nature* 426, 803–809.

Harada, S., Watanabe, Y., Takeuchi, K., Suzuki, T., Katayama, T., Takebe, Y., Saito, I., and Miyamura, T. (1991). Expression of processed core protein of hepatitis C virus in mammalian cells. *J. Virol.* 65, 3015–3021.

Harris, C., Herker, E., Farese, R. V. Jr., and Ott, M. (2011). Hepatitis C Virus Core Protein Decreases Lipid Droplet Turnover: a mechanism for core-induced steatosis. *J. Biol. Chem.* 286, 42615–42625.

Havel, R. J. (2000). Remnant lipoproteins as therapeutic targets. *Curr. Opin. Lipidol.* 11, 615–620.

Herker, E., Harris, C., Hernandez, C., Carpentier, A., Kaehlcke, K., Rosenberg, A. R., Farese, R. V. Jr., and Ott, M. (2010). Efficient hepatitis C virus particle formation requires diacylglycerol acyltransferase-1. *Nat. Med.* 16, 1295–1298.

Herz, J., Chen, Y., Masiulis, I., and Zhou, L. (2009). Expanding functions of lipoprotein receptors. *J. Lipid Res.* 50(Suppl.), S287–S292.

Hicham Alaoui-Ismaili, M., Gervais, C., Brunette, S., Gouin, G., Hamel, M., Rando, R. F., and Bedard, J. (2000). A novel high throughput screening assay for HCV NS3 helicase activity. *Antiviral Res.* 46, 181–193.

Hijikata, M., Kato, N., Ootsuyama, Y., Nakagawa, M., and Shimotohno, K. (1991). Gene mapping of the putative structural region of the hepatitis C virus genome by in vitro processing analysis. *Proc. Natl. Acad. Sci. U.S.A.* 88, 5547–5551.

Hijikata, M., Shimizu, Y. K., Kato, H., Iwamoto, A., Shih, J. W., Alter, H. J., Purcell, R. H., and Yoshikura, H. (1993). Equilibrium centrifugation studies of hepatitis C virus: evidence for circulating immune complexes. *J. Virol.* 67, 1953–1958.

Hishiki, T., Shimizu, Y., Tobita, R., Sugiyama, K., Ogawa, K., Funami, K., Ohsaki, Y., Fujimoto, T., Takaku, H., Wakita, T., Baumert, T. F., Miyanari, Y., and Shimotohno, K. (2010). Infectivity of hepatitis C virus is influenced by association with apolipoprotein E isoforms. *J. Virol.* 84, 12048–12057.

Hofmann, W. P., and Zeuzem, S. (2011). A new standard of care for the treatment of chronic HCV infection. *Nat. Rev. Gastroenterol. Hepatol.* 8, 257–264.

Hope, R. G., and McLauchlan, J. (2000). Sequence motifs required for lipid droplet association and protein stability are unique to the hepatitis C virus core protein. *J. Gen. Virol.* 81, 1913–1925.

Hope, R. G., Murphy, D. J., and Mclauchlan, J. (2002). The domains required to direct core proteins of hepatitis C virus and GB virus-B to lipid droplets share common features with plant oleosin proteins. *J. Biol. Chem.* 277, 4261–4270.

Hopkins, S., Scorneaux, B., Huang, Z., Murray, M. G., Wring, S., Smitley, C., Harris, R., Erdmann, F., Fischer, G., and Ribeill, Y. (2010). SCY-635, a novel nonimmunosuppressive analog of cyclosporine that exhibits potent inhibition of hepatitis C virus RNA replication in vitro. *Antimicrob. Agents Chemother.* 54, 660–672.

Horton, J. D., Goldstein, J. L., and Brown, M. S. (2002). SREBPs: activators of the complete program of cholesterol and fatty acid synthesis in the liver. *J. Clin. Invest.* 109, 1125–1131.

Hsu, M., Zhang, J., Flint, M., Logvinoff, C., Cheng-Mayer, C., Rice, C. M., and Mckeating, J. A. (2003). Hepatitis C virus glycoproteins mediate pH-dependent cell entry of pseudotyped retroviral particles. *Proc. Natl. Acad. Sci. U.S.A.* 100, 7271–7276.

Hsu, N. Y., Ilnytska, O., Belov, G., Santiana, M., Chen, Y. H., Takvorian, P. M., Pau, C., Van Der Schaar, H., Kaushik-Basu, N., Balla, T., Cameron, C. E., Ehrenfeld, E., Van Kuppeveld, F. J., and Altan-Bonnet, N. (2010). Viral reorganization of the secretory pathway generates distinct organelles for RNA replication. *Cell* 141, 799–811.

Huang, H., Sun, F., Owen, D. M., Li, W., Chen, Y., Gale, M. Jr., and Ye, J. (2007). Hepatitis C virus production by human hepatocytes dependent on assembly and secretion of very low-density lipoproteins. *Proc. Natl. Acad. Sci. U.S.A.* 104, 5848–5853.

Hussy, P., Langen, H., Mous, J., and Jacobsen, H. (1996). Hepatitis C virus core protein: carboxy-terminal boundaries of two processed species suggest cleavage by a signal peptide peptidase. *Virology* 224, 93–104.

Ikeda, M., Yi, M., Li, K., and Lemon, S. M. (2002). Selectable subgenomic and genome-length dicistronic RNAs derived from an infectious molecular clone of the HCV-N strain of hepatitis C virus replicate efficiently in cultured Huh7 cells. *J. Virol.* 76, 2997–3006.

Ilyin, G. P., Rialland, M., Glaise, D., and Guguen-Guillouzo, C. (1999). Identification of a novel Skp2-like mammalian protein containing F-box and leucine-rich repeats. *FEBS Lett.* 459, 75–79.

Inoue, K., Sekiyama, K., Yamada, M., Watanabe, T., Yasuda, H., and Yoshiba, M. (2003). Combined interferon alpha2b and cyclosporin A in the treatment of chronic hepatitis C: controlled trial. *J. Gastroenterol.* 38, 567–572.

Ishii, N., Watashi, K., Hishiki, T., Goto, K., Inoue, D., Hijikata, M., Wakita, T., Kato, N., and Shimotohno, K. (2006). Diverse effects of cyclosporine on hepatitis C virus strain replication. *J. Virol.* 80, 4510–4520.

Ito, M., Masumi, A., Mochida, K., Kukihara, H., Moriishi, K., Matsuura, Y., Yamaguchi, K., and Mizuochi, T. (2010). Peripheral B cells may serve as a reservoir for persistent hepatitis C virus infection. *J. Innate Immun.* 2, 607–617.

Jacobson, I. M., Cacoub, P., Dal Maso, L., Harrison, S. A., and Younossi, Z. M. (2010). Manifestations of chronic hepatitis C virus infection beyond the liver. *Clin. Gastroenterol. Hepatol.* 8, 1017–1029.

Jiang, J., and Luo, G. (2009). Apolipoprotein E but not B is required for the formation of infectious hepatitis C virus particles. *J. Virol.* 83, 12680–12691.

Jirasko, V., Montserret, R., Appel, N., Janvier, A., Eustachi, L., Brohm, C., Steinmann, E., Pietschmann, T., Penin, F., and Bartenschlager, R. (2008). Structural and functional characterization of nonstructural protein 2 for its role in hepatitis C virus assembly. *J. Biol. Chem.* 283, 28546–28562.

Jones, C. T., Murray, C. L., Eastman, D. K., Tassello, J., and Rice, C. M. (2007). Hepatitis C virus p7 and NS2 proteins are essential for production of infectious virus. *J. Virol.* 81, 8374–8383.

Kapadia, S. B., and Chisari, F. V. (2005). Hepatitis C virus RNA replication is regulated by host geranylgeranylation and fatty acids. *Proc. Natl. Acad. Sci. U.S.A.* 102, 2561–2566.

Kasama, Y., Sekiguchi, S., Saito, M., Tanaka, K., Satoh, M., Kuwahara, K., Sakaguchi, N., Takeya, M., Hiasa, Y., Kohara, M., and Tsukiyama-Kohara, K. (2010). Persistent expression of the full genome of hepatitis C virus in B cells induces spontaneous development of B-cell lymphomas in vivo. *Blood* 116, 4926–4933.

Kaul, A., Stauffer, S., Berger, C., Pertel, T., Schmitt, J., Kallis, S., Zayas, M., Lohmann, V., Luban, J., and Bartenschlager, R. (2009). Essential role of cyclophilin A for hepatitis C virus replication and virus production and possible link to polyprotein cleavage kinetics. *PLoS Pathog.* 5, e1000546. doi:10.1371/journal.ppat.1000546

Kawano, M., Kumagai, K., Nishijima, M., and Hanada, K. (2006). Efficient trafficking of ceramide from the endoplasmic reticulum to the Golgi apparatus requires a VAMP-associated protein-interacting FFAT motif of CERT. *J. Biol. Chem.* 281, 30279–30288.

Koch, J. O., Lohmann, V., Herian, U., and Bartenschlager, R. (1996). In vitro studies on the activation of the hepatitis C virus NS3 proteinase by the NS4A cofactor. *Virology* 221, 54–66.

Kockx, M., Jessup, W., and Kritharides, L. (2010). Cyclosporin A and atherosclerosis – cellular pathways in atherogenesis. *Pharmacol. Ther.* 128, 106–118.

Koike, K., Tsutsumi, T., Yotsuyanagi, H., and Moriya, K. (2010). Lipid metabolism and liver disease in hepatitis C viral infection. *Oncology* 78(Suppl. 1), 24–30.

Krieger, N., Lohmann, V., and Bartenschlager, R. (2001). Enhancement of hepatitis C virus RNA replication by cell culture-adaptive mutations. *J. Virol.* 75, 4614–4624.

Kukihara, H., Moriishi, K., Taguwa, S., Tani, H., Abe, T., Mori, Y., Suzuki, T., Fukuhara, T., Taketomi, A., Maehara, Y., and Matsuura, Y. (2009). Human VAP-C negatively regulates hepatitis C virus propagation. *J. Virol.* 83, 7959–7969.

Kumagai, K., Yasuda, S., Okemoto, K., Nishijima, M., Kobayashi, S., and Hanada, K. (2005). CERT mediates intermembrane transfer of various molecular species of ceramides. *J. Biol. Chem.* 280, 6488–6495.

Li, K., Foy, E., Ferreon, J. C., Nakamura, M., Ferreon, A. C., Ikeda, M., Ray, S. C., Gale, M. Jr., and Lemon, S. M. (2005a). Immune evasion by hepatitis C virus NS3/4A protease-mediated cleavage of the Toll-like receptor 3 adaptor protein TRIF. *Proc. Natl. Acad. Sci. U.S.A.* 102, 2992–2997.

Li, X. D., Sun, L., Seth, R. B., Pineda, G., and Chen, Z. J. (2005b). Hepatitis C virus protease NS3/4A cleaves mitochondrial antiviral signaling protein off the mitochondria to evade innate immunity. *Proc. Natl. Acad. Sci. U.S.A.* 102, 17717–17722.

Li, Q., Brass, A. L., Ng, A., Hu, Z., Xavier, R. J., Liang, T. J., and Elledge, S. J. (2009). A genome-wide genetic screen for host factors required for hepatitis C virus propagation. *Proc. Natl. Acad. Sci. U.S.A.* 106, 16410–16415.

Li, X., Lonard, D. M., Jung, S. Y., Malovannaya, A., Feng, Q., Qin, J., Tsai, S. Y., Tsai, M. J., and O'malley, B. W. (2006). The SRC-3/AIB1 coactivator is degraded in a ubiquitin- and ATP-independent manner by the REGgamma proteasome. *Cell* 124, 381–392.

Lim, Y. S., and Hwang, S. B. (2011). Hepatitis C virus NS5A protein interacts with phosphatidylinositol 4-kinase type IIIalpha and regulates viral propagation. *J. Biol. Chem.* 286, 11290–11298.

Lindenbach, B. D., Evans, M. J., Syder, A. J., Wolk, B., Tellinghuisen, T. L., Liu, C. C., Maruyama, T., Hynes, R. O., Burton, D. R., Mckeating, J. A., and Rice, C. M. (2005). Complete replication of hepatitis C virus in cell culture. *Science* 309, 623–626.

Lindenbach, B. D., Meuleman, P., Ploss, A., Vanwolleghem, T., Syder, A. J., Mckeating, J. A., Lanford, R. E., Feinstone, S. M., Major, M. E., Leroux-Roels, G., and Rice, C. M. (2006). Cell culture-grown hepatitis C virus is infectious in vivo and can be recultured in vitro. *Proc. Natl. Acad. Sci. U.S.A.* 103, 3805–3809.

Liu, J., Farmer, J. D. Jr., Lane, W. S., Friedman, J., Weissman, I., and Schreiber, S. L. (1991). Calcineurin is a common target of cyclophilin-cyclosporin A and FKBP-FK506 complexes. *Cell* 66, 807–815.

Loewen, C. J., Roy, A., and Levine, T. P. (2003). A conserved ER targeting motif in three families of lipid binding proteins and in Opi1p binds VAP. *EMBO J.* 22, 2025–2035.

Lohmann, V., Korner, F., Dobierzewska, A., and Bartenschlager, R. (2001). Mutations in hepatitis C virus RNAs conferring cell culture adaptation. *J. Virol.* 75, 1437–1449.

Lohmann, V., Korner, F., Koch, J., Herian, U., Theilmann, L., and Bartenschlager, R. (1999). Replication of subgenomic hepatitis C virus RNAs in a hepatoma cell line. *Science* 285, 110–113.

Loo, Y. M., Fornek, J., Crochet, N., Bajwa, G., Perwitasari, O., Martinez-Sobrido, L., Akira, S., Gill, M. A., Garcia-Sastre, A., Katze, M. G., and Gale, M. Jr. (2008). Distinct RIG-I and MDA5 signaling by RNA viruses in innate immunity. *J. Virol.* 82, 335–345.

Loo, Y. M., Owen, D. M., Li, K., Erickson, A. K., Johnson, C. L., Fish, P. M., Carney, D. S., Wang, T., Ishida, H., Yoneyama, M., Fujita, T., Saito, T., Lee, W. M., Hagedorn, C. H., Lau, D. T., Weinman, S. A., Lemon, S. M., and Gale, M. Jr. (2006). Viral and therapeutic control of IFN-beta promoter stimulator 1 during hepatitis C virus infection. *Proc. Natl. Acad. Sci. U.S.A.* 103, 6001–6006.

Lorenz, I. C., Marcotrigiano, J., Dentzer, T. G., and Rice, C. M. (2006). Structure of the catalytic domain of the hepatitis C virus NS2-3 protease. *Nature* 442, 831–835.

Ma, S., Boerner, J. E., Tiongyip, C., Weidmann, B., Ryder, N. S., Cooreman, M. P., and Lin, K. (2006). NIM811, a cyclophilin inhibitor, exhibits potent in vitro activity against hepatitis C virus alone or in combination with alpha interferon. *Antimicrob. Agents Chemother.* 50, 2976–2982.

Maga, G., Gemma, S., Fattorusso, C., Locatelli, G. A., Butini, S., Persico, M., Kukreja, G., Romano, M. P., Chiasserini, L., Savini, L., Novellino, E., Nacci, V., Spadari, S., and Campiani, G. (2005). Specific targeting of hepatitis C virus NS3 RNA helicase. Discovery of the potent and selective competitive nucleotide-mimicking inhibitor QU663. *Biochemistry* 44, 9637–9644.

Mannova, P., Fang, R., Wang, H., Deng, B., Mcintosh, M. W., Hanash, S. M., and Beretta, L. (2006). Modification of host lipid raft proteome upon hepatitis C virus replication. *Mol. Cell Proteomics* 5, 2319–2325.

Masaki, T., Suzuki, R., Murakami, K., Aizaki, H., Ishii, K., Murayama, A., Date, T., Matsuura, Y., Miyamura, T., Wakita, T., and Suzuki, T. (2008). Interaction of hepatitis C virus nonstructural protein 5A with core protein is critical for the production of infectious virus particles. *J. Virol.* 82, 7964–7976.

Matto, M., Rice, C. M., Aroeti, B., and Glenn, J. S. (2004). Hepatitis C virus core protein associates with detergent-resistant membranes distinct from classical plasma membrane rafts. *J. Virol.* 78, 12047–12053.

McLauchlan, J., Lemberg, M. K., Hope, G., and Martoglio, B. (2002). Intramembrane proteolysis promotes trafficking of hepatitis C virus core protein to lipid droplets. *EMBO J.* 21, 3980–3988.

Meertens, L., Bertaux, C., and Dragic, T. (2006). Hepatitis C virus entry requires a critical postinternalization step and delivery to early endosomes via clathrin-coated vesicles. *J. Virol.* 80, 11571–11578.

Merz, A., Long, G., Hiet, M. S., Brugger, B., Chlanda, P., Andre, P., Wieland, F., Krijnse-Locker, J., and Bartenschlager, R. (2011). Biochemical and morphological properties of hepatitis C virus particles and determination of their lipidome. *J. Biol. Chem.* 286, 3018–30132.

Miyanari, Y., Atsuzawa, K., Usuda, N., Watashi, K., Hishiki, T., Zayas, M., Bartenschlager, R., Wakita, T., Hijikata, M., and Shimotohno, K. (2007). The lipid droplet is an important organelle for hepatitis C virus production. *Nat. Cell Biol.* 9, 1089–1097.

Miyoshi, H., Moriya, K., Tsutsumi, T., Shinzawa, S., Fujie, H., Shintani, Y., Fujinaga, H., Goto, K., Todoroki, T., Suzuki, T., Miyamura, T., Matsuura, Y., Yotsuyanagi, H., and

Koike, K. (2011). Pathogenesis of lipid metabolism disorder in hepatitis C: polyunsaturated fatty acids counteract lipid alterations induced by the core protein. *J. Hepatol.* 54, 432–438.

Monazahian, M., Bohme, I., Bonk, S., Koch, A., Scholz, C., Grethe, S., and Thomssen, R. (1999). Low density lipoprotein receptor as a candidate receptor for hepatitis C virus. *J. Med. Virol.* 57, 223–229.

Moriishi, K., Mochizuki, R., Moriya, K., Miyamoto, H., Mori, Y., Abe, T., Murata, S., Tanaka, K., Miyamura, T., Suzuki, T., Koike, K., and Matsuura, Y. (2007). Critical role of PA28gamma in hepatitis C virus-associated steatogenesis and hepatocarcinogenesis. *Proc. Natl. Acad. Sci. U.S.A.* 104, 1661–1666.

Moriishi, K., Okabayashi, T., Nakai, K., Moriya, K., Koike, K., Murata, S., Chiba, T., Tanaka, K., Suzuki, R., Suzuki, T., Miyamura, T., and Matsuura, Y. (2003). Proteasome activator PA28gamma-dependent nuclear retention and degradation of hepatitis C virus core protein. *J. Virol.* 77, 10237–10249.

Moriishi, K., Shoji, I., Mori, Y., Suzuki, R., Suzuki, T., Kataoka, C., and Matsuura, Y. (2010). Involvement of PA28gamma in the propagation of hepatitis C virus. *Hepatology* 52, 411–420.

Moriya, K., Nakagawa, K., Santa, T., Shintani, Y., Fujie, H., Miyoshi, H., Tsutsumi, T., Miyazawa, T., Ishibashi, K., Horie, T., Imai, K., Todoroki, T., Kimura, S., and Koike, K. (2001). Oxidative stress in the absence of inflammation in a mouse model for hepatitis C virus-associated hepatocarcinogenesis. *Cancer Res.* 61, 4365–4670.

Moriya, K., Yotsuyanagi, H., Shintani, Y., Fujie, H., Ishibashi, K., Matsuura, Y., Miyamura, T., and Koike, K. (1997). Hepatitis C virus core protein induces hepatic steatosis in transgenic mice. *J. Gen. Virol.* 78 (Pt 7), 1527–1531.

Najda-Bernatowicz, A., Krawczyk, M., Stankiewicz-Drogon, A., Bretner, M., and Boguszewska-Chachulska, A. M. (2010). Studies on the anti-hepatitis C virus activity of newly synthesized tropolone derivatives: identification of NS3 helicase inhibitors that specifically inhibit subgenomic HCV replication. *Bioorg. Med. Chem.* 18, 5129–5136.

Nielsen, S. U., Bassendine, M. F., Burt, A. D., Martin, C., Pumeechockchai, W., and Toms, G. L. (2006). Association between hepatitis C virus and very-low-density lipoprotein (VLDL)/LDL analyzed in iodixanol density gradients. *J. Virol.* 80, 2418–2428.

Nishimura, Y., Hayashi, M., Inada, H., and Tanaka, T. (1999). Molecular cloning and characterization of mammalian homologues of vesicle-associated membrane protein-associated (VAMP-associated) proteins. *Biochem. Biophys. Res. Commun.* 254, 21–26.

Nunez, O., Fernandez-Martinez, A., Majano, P. L., Apolinario, A., Gomez-Gonzalo, M., Benedicto, I., Lopez-Cabrera, M., Bosca, L., Clemente, G., Garcia-Monzon, C., and Martin-Sanz, P. (2004). Increased intrahepatic cyclooxygenase 2, matrix metalloproteinase 2, and matrix metalloproteinase 9 expression is associated with progressive liver disease in chronic hepatitis C virus infection: role of viral core and NS5A proteins. *Gut* 53, 1665–1672.

Ogino, T., Fukuda, H., Imajoh-Ohmi, S., Kohara, M., and Nomoto, A. (2004). Membrane binding properties and terminal residues of the mature hepatitis C virus capsid protein in insect cells. *J. Virol.* 78, 11766–11777.

Ohata, K., Hamasaki, K., Toriyama, K., Matsumoto, K., Saeki, A., Yanagi, K., Abiru, S., Nakagawa, Y., Shigeno, M., Miyazoe, S., Ichikawa, T., Ishikawa, H., Nakao, K., and Eguchi, K. (2003). Hepatic steatosis is a risk factor for hepatocellular carcinoma in patients with chronic hepatitis C virus infection. *Cancer* 97, 3036–3043.

Okamoto, K., Mori, Y., Komoda, Y., Okamoto, T., Okochi, M., Takeda, M., Suzuki, T., Moriishi, K., and Matsuura, Y. (2008). Intramembrane processing by signal peptide peptidase regulates the membrane localization of hepatitis C virus core protein and viral propagation. *J. Virol.* 82, 8349–8361.

Okamoto, K., Moriishi, K., Miyamura, T., and Matsuura, Y. (2004). Intramembrane proteolysis and endoplasmic reticulum retention of hepatitis C virus core protein. *J. Virol.* 78, 6370–6380.

Okamoto, T., Nishimura, Y., Ichimura, T., Suzuki, K., Miyamura, T., Suzuki, T., Moriishi, K., and Matsuura, Y. (2006). Hepatitis C virus RNA replication is regulated by FKBP8 and Hsp90. *EMBO J.* 25, 5015–5025.

Okuda, M., Li, K., Beard, M. R., Showalter, L. A., Scholle, F., Lemon, S. M., and Weinman, S. A. (2002). Mitochondrial injury, oxidative stress, and antioxidant gene expression are induced by hepatitis C virus core protein. *Gastroenterology* 122, 366–375.

Oomens, A. G., Bevis, K. P., and Wertz, G. W. (2006). The cytoplasmic tail of the human respiratory syncytial virus F protein plays critical roles in cellular localization of the F protein and infectious progeny production. *J. Virol.* 80, 10465–10477.

Peretti, D., Dahan, N., Shimoni, E., Hirschberg, K., and Lev, S. (2008). Coordinated lipid transfer between the endoplasmic reticulum and the Golgi complex requires the VAP proteins and is essential for Golgi-mediated transport. *Mol. Biol. Cell* 19, 3871–3884.

Perlemuter, G., Sabile, A., Letteron, P., Vona, G., Topilco, A., Chretien, Y., Koike, K., Pessayre, D., Chapman, J., Barba, G., and Brechot, C. (2002). Hepatitis C virus core protein inhibits microsomal triglyceride transfer protein activity and very low density lipoprotein secretion: a model of viral-related steatosis. *FASEB J.* 16, 185–194.

Pietschmann, T., Kaul, A., Koutsoudakis, G., Shavinskaya, A., Kallis, S., Steinmann, E., Abid, K., Negro, F., Dreux, M., Cosset, F. L., and Bartenschlager, R. (2006). Construction and characterization of infectious intragenotypic and intergenotypic hepatitis C virus chimeras. *Proc. Natl. Acad. Sci. U.S.A.* 103, 7408–7413.

Pietschmann, T., Lohmann, V., Kaul, A., Krieger, N., Rinck, G., Rutter, G., Strand, D., and Bartenschlager, R. (2002). Persistent and transient replication of full-length hepatitis C virus genomes in cell culture. *J. Virol.* 76, 4008–4021.

Pileri, P., Uematsu, Y., Campagnoli, S., Galli, G., Falugi, F., Petracca, R., Weiner, A. J., Houghton, M., Rosa, D., Grandi, G., and Abrignani, S. (1998). Binding of hepatitis C virus to CD81. *Science* 282, 938–941.

Ploss, A., Evans, M. J., Gaysinskaya, V. A., Panis, M., You, H., De Jong, Y. P., and Rice, C. M. (2009). Human occludin is a hepatitis C virus entry factor required for infection of mouse cells. *Nature* 457, 882–886.

Popescu, C. I., Callens, N., Trinel, D., Roingeard, P., Moradpour, D., Descamps, V., Duverlie, G., Penin, F., Heliot, L., Rouille, Y., and Dubuisson, J. (2011). NS2 protein of hepatitis C virus interacts with structural and non-structural proteins towards virus assembly. *PLoS Pathog.* 7, e1001278. doi:10.1371/journal.ppat.1001278

Pumeechockchai, W., Bevitt, D., Agarwal, K., Petropoulou, T., Langer, B. C., Belohradsky, B., Bassendine, M. F., and Toms, G. L. (2002). Hepatitis C virus particles of different density in the blood of chronically infected immunocompetent and immunodeficient patients: implications for virus clearance by antibody. *J. Med. Virol.* 68, 335–342.

Rahfeld, J. U., Schierhorn, A., Mann, K., and Fischer, G. (1994). A novel peptidyl-prolyl cis/trans isomerase from *Escherichia coli*. *FEBS Lett.* 343, 65–69.

Randall, G., Panis, M., Cooper, J. D., Tellinghuisen, T. L., Sukhodolets, K. E., Pfeffer, S., Landthaler, M., Landgraf, P., Kan, S., Lindenbach, B. D., Chien, M., Weir, D. B., Russo, J. J., Ju, J., Brownstein, M. J., Sheridan, R., Sander, C., Zavolan, M., Tuschl, T., and Rice, C. M. (2007). Cellular cofactors affecting hepatitis C virus infection and replication. *Proc. Natl. Acad. Sci. U.S.A.* 104, 12884–12889.

Reiss, S., Rebhan, I., Backes, P., Romero-Brey, I., Erfle, H., Matula, P., Kaderali, L., Poenisch, M., Blankenburg, H., Hiet, M. S., Longerich, T., Diehl, S., Ramirez, F., Balla, T., Rohr, K., Kaul, A., Buhler, S., Pepperkok, R., Lengauer, T., Albrecht, M., Eils, R., Schirmacher, P., Lohmann, V., and Bartenschlager, R. (2011). Recruitment and activation of a lipid kinase by hepatitis C virus NS5A is essential for integrity of the membranous replication compartment. *Cell Host Microbe* 9, 32–45.

Ridgway, N. D., Dawson, P. A., Ho, Y. K., Brown, M. S., and Goldstein, J. L. (1992). Translocation of oxysterol binding protein to Golgi apparatus triggered by ligand binding. *J. Cell Biol.* 116, 307–319.

Rubbia-Brandt, L., Quadri, R., Abid, K., Giostra, E., Male, P. J., Mentha, G., Spahr, L., Zarski, J. P., Borisch, B., Hadengue, A., and Negro, F. (2000). Hepatocyte steatosis is a cytopathic effect of hepatitis C virus genotype 3. *J. Hepatol.* 33, 106–115.

Sainz, B. Jr., Barretto, N., Martin, D. N., Hiraga, N., Imamura, M., Hussain, S., Marsh, K. A., Yu, X., Chayama, K., Alrefai, W. A., and Uprichard, S. L. (2012). Identification of the Niemann-Pick C1-like 1 cholesterol absorption receptor as a new hepatitis C virus entry factor. *Nat. Med.* doi: 10.1038/nm.2581

Sakamoto, H., Okamoto, K., Aoki, M., Kato, H., Katsume, A., Ohta, A., Tsukuda, T., Shimma, N., Aoki, Y., Arisawa, M., Kohara, M., and Sudoh, M. (2005). Host sphingolipid biosynthesis as a target for hepatitis

C virus therapy. *Nat. Chem. Biol.* 1, 333–337.

Santolini, E., Migliaccio, G., and La Monica, N. (1994). Biosynthesis and biochemical properties of the hepatitis C virus core protein. *J. Virol.* 68, 3631–3641.

Santolini, E., Pacini, L., Fipaldini, C., Migliaccio, G., and Monica, N. (1995). The NS2 protein of hepatitis C virus is a transmembrane polypeptide. *J. Virol.* 69, 7461–7471.

Scarselli, E., Ansuini, H., Cerino, R., Roccasecca, R. M., Acali, S., Filocamo, G., Traboni, C., Nicosia, A., Cortese, R., and Vitelli, A. (2002). The human scavenger receptor class B type I is a novel candidate receptor for the hepatitis C virus. *EMBO J.* 21, 5017–5025.

Schiene-Fischer, C., Habazettl, J., Schmid, F. X., and Fischer, G. (2002). The hsp70 chaperone DnaK is a secondary amide peptide bond cis-trans isomerase. *Nat. Struct. Biol.* 9, 419–424.

Shavinskaya, A., Boulant, S., Penin, F., Mclauchlan, J., and Bartenschlager, R. (2007). The lipid droplet binding domain of hepatitis C virus core protein is a major determinant for efficient virus assembly. *J. Biol. Chem.* 282, 37158–37169.

Shi, S. T., Lee, K. J., Aizaki, H., Hwang, S. B., and Lai, M. M. (2003). Hepatitis C virus RNA replication occurs on a detergent-resistant membrane that cofractionates with caveolin-2. *J. Virol.* 77, 4160–4168.

Siekierka, J. J., Hung, S. H., Poe, M., Lin, C. S., and Sigal, N. H. (1989a). A cytosolic binding protein for the immunosuppressant FK506 has peptidyl-prolyl isomerase activity but is distinct from cyclophilin. *Nature* 341, 755–757.

Siekierka, J. J., Staruch, M. J., Hung, S. H., and Sigal, N. H. (1989b). FK-506, a potent novel immunosuppressive agent, binds to a cytosolic protein which is distinct from the cyclosporin A-binding protein, cyclophilin. *J. Immunol.* 143, 1580–1583.

Skehel, P. A., Martin, K. C., Kandel, E. R., and Bartsch, D. (1995). A VAMP-binding protein from Aplysia required for neurotransmitter release. *Science* 269, 1580–1583.

Soriano, V., Peters, M. G., and Zeuzem, S. (2009). New therapies for hepatitis C virus infection. *Clin. Infect. Dis.* 48, 313–320.

Spik, G., Haendler, B., Delmas, O., Mariller, C., Chamoux, M., Maes, P., Tartar, A., Montreuil, J., Stedman, K., Kocher, H. P., Keller, R., Hiestad, P. C., and Movva, N. R. (1991). A novel secreted cyclophilin-like protein (SCYLP). *J. Biol. Chem.* 266, 10735–10738.

Steinmann, E., Penin, F., Kallis, S., Patel, A. H., Bartenschlager, R., and Pietschmann, T. (2007). Hepatitis C virus p7 protein is crucial for assembly and release of infectious virions. *PLoS Pathog.* 3, e103. doi:10.1371/journal.ppat.0030103

Sumpter, R. Jr., Loo, Y. M., Foy, E., Li, K., Yoneyama, M., Fujita, T., Lemon, S. M., and Gale, M. Jr. (2005). Regulating intracellular antiviral defense and permissiveness to hepatitis C virus RNA replication through a cellular RNA helicase, RIG-I. *J. Virol.* 79, 2689–2699.

Suzuki, R., Moriishi, K., Fukuda, K., Shirakura, M., Ishii, K., Shoji, I., Wakita, T., Miyamura, T., Matsuura, Y., and Suzuki, T. (2009). Proteasomal turnover of hepatitis C virus core protein is regulated by two distinct mechanisms: a ubiquitin-dependent mechanism and a ubiquitin-independent but PA28gamma-dependent mechanism. *J. Virol.* 83, 2389–2392.

Tai, A. W., Benita, Y., Peng, L. F., Kim, S. S., Sakamoto, N., Xavier, R. J., and Chung, R. T. (2009). A functional genomic screen identifies cellular cofactors of hepatitis C virus replication. *Cell Host Microbe* 5, 298–307.

Tai, A. W., and Salloum, S. (2011). The role of the phosphatidylinositol 4-kinase PI4KA in hepatitis C virus-induced host membrane rearrangement. *PLoS ONE* 6, e26300. doi:10.1371/journal.pone.0026300

Takikawa, S., Ishii, K., Aizaki, H., Suzuki, T., Asakura, H., Matsuura, Y., and Miyamura, T. (2000). Cell fusion activity of hepatitis C virus envelope proteins. *J. Virol.* 74, 5066–5074.

Targett-Adams, P., Hope, G., Boulant, S., and Mclauchlan, J. (2008). Maturation of hepatitis C virus core protein by signal peptide peptidase is required for virus production. *J. Biol. Chem.* 283, 16850–16859.

Thomssen, R., Bonk, S., Propfe, C., Heermann, K. H., Kochel, H. G., and Uy, A. (1992). Association of hepatitis C virus in human sera with beta-lipoprotein. *Med. Microbiol. Immunol.* 181, 293–300.

Thomssen, R., Bonk, S., and Thiele, A. (1993). Density heterogeneities of hepatitis C virus in human sera due to the binding of beta-lipoproteins and immunoglobulins. *Med. Microbiol. Immunol.* 182, 329–334.

Tory, R., Sachs-Barrable, K., Hill, J. S., and Wasan, K. M. (2008). Cyclosporine A and rapamycin induce in vitro cholesteryl ester transfer protein activity, and suppress lipoprotein lipase activity in human plasma. *Int. J. Pharm.* 358, 219–223.

Tripathi, L. P., Kataoka, C., Taguwa, S., Moriishi, K., Mori, Y., Matsuura, Y., and Mizuguchi, K. (2010). Network based analysis of hepatitis C virus core and NS4B protein interactions. *Mol. Biosyst.* 6, 2539–2553.

Trotard, M., Lepere-Douard, C., Regeard, M., Piquet-Pellorce, C., Lavillette, D., Cosset, F. L., Gripon, P., and Le Seyec, J. (2009). Kinases required in hepatitis C virus entry and replication highlighted by small interference RNA screening. *FASEB J.* 23, 3780–3789.

Tscherne, D. M., Jones, C. T., Evans, M. J., Lindenbach, B. D., Mckeating, J. A., and Rice, C. M. (2006). Time- and temperature-dependent activation of hepatitis C virus for low-pH-triggered entry. *J. Virol.* 80, 1734–1741.

Tsukiyama-Kohara, K., Iizuka, N., Kohara, M., and Nomoto, A. (1992). Internal ribosome entry site within hepatitis C virus RNA. *J. Virol.* 66, 1476–1483.

Tsutsumi, T., Suzuki, T., Shimoike, T., Suzuki, R., Moriya, K., Shintani, Y., Fujie, H., Matsuura, Y., Koike, K., and Miyamura, T. (2002). Interaction of hepatitis C virus core protein with retinoid X receptor alpha modulates its transcriptional activity. *Hepatology* 35, 937–946.

Tu, H., Gao, L., Shi, S. T., Taylor, D. R., Yang, T., Mircheff, A. K., Wen, Y., Gorbalenya, A. E., Hwang, S. B., and Lai, M. M. (1999). Hepatitis C virus RNA polymerase and NS5A complex with a SNARE-like protein. *Virology* 263, 30–41.

Vaillancourt, F. H., Pilote, L., Cartier, M., Lippens, J., Liuzzi, M., Bethell, R. C., Cordingley, M. G., and Kukolj, G. (2009). Identification of a lipid kinase as a host factor involved in hepatitis C virus RNA replication. *Virology* 387, 5–10.

Vieyres, G., Thomas, X., Descamps, V., Duverlie, G., Patel, A. H., and Dubuisson, J. (2010). Characterization of the envelope glycoproteins associated with infectious hepatitis C virus. *J. Virol.* 84, 10159–10168.

Voisset, C., Lavie, M., Helle, F., Op De Beeck, A., Bilheu, A., Bertrand-Michel, J., Terce, F., Cocquerel, L., Wychowski, C., Vu-Dac, N., and Dubuisson, J. (2008). Ceramide enrichment of the plasma membrane induces CD81 internalization and inhibits hepatitis C virus entry. *Cell. Microbiol.* 10, 606–617.

Wakita, T., Pietschmann, T., Kato, T., Date, T., Miyamoto, M., Zhao, Z., Murthy, K., Habermann, A., Krausslich, H. G., Mizokami, M., Bartenschlager, R., and Liang, T. J. (2005). Production of infectious hepatitis C virus in tissue culture from a cloned viral genome. *Nat. Med.* 11, 791–796.

Wang, C., Gale, M. Jr., Keller, B. C., Huang, H., Brown, M. S., Goldstein, J. L., and Ye, J. (2005a). Identification of FBL2 as a geranylgeranylated cellular protein required for hepatitis C virus RNA replication. *Mol. Cell* 18, 425–434.

Wang, P. Y., Weng, J., and Anderson, R. G. (2005b). OSBP is a cholesterol-regulated scaffolding protein in control of ERK 1/2 activation. *Science* 307, 1472–1476.

Watashi, K., Hijikata, M., Hosaka, M., Yamaji, M., and Shimotohno, K. (2003). Cyclosporin A suppresses replication of hepatitis C virus genome in cultured hepatocytes. *Hepatology* 38, 1282–1288.

Watashi, K., Ishii, N., Hijikata, M., Inoue, D., Murata, T., Miyanari, Y., and Shimotohno, K. (2005). Cyclophilin B is a functional regulator of hepatitis C virus RNA polymerase. *Mol. Cell* 19, 111–122.

Wolins, N. E., Brasaemle, D. L., and Bickel, P. E. (2006). A proposed model of fat packaging by exchangeable lipid droplet proteins. *FEBS Lett.* 580, 5484–5491.

Wolk, B., Sansonno, D., Krausslich, H. G., Dammacco, F., Rice, C. M., Blum, H. E., and Moradpour, D. (2000). Subcellular localization, stability, and trans-cleavage competence of the hepatitis C virus NS3-NS4A complex expressed in tetracycline-regulated cell lines. *J. Virol.* 74, 2293–2304.

Wozniak, A. L., Griffin, S., Rowlands, D., Harris, M., Yi, M., Lemon, S. M., and Weinman, S. A. (2010). Intracellular proton conductance of the hepatitis C virus p7 protein and its contribution to infectious virus production. *PLoS Pathog.* 6, e1001087. doi:10.1371/journal.ppat.1001087

Yamaga, A. K., and Ou, J. H. (2002). Membrane topology of the hepatitis C virus NS2 protein. *J. Biol. Chem.* 277, 33228–33234.

Yang, F., Robotham, J. M., Nelson, H. B., Irsigler, A., Kenworthy, R., and Tang, H. (2008). Cyclophilin A is an essential cofactor for hepatitis C virus infection and the principal mediator of cyclosporine resistance in vitro. *J. Virol.* 82, 5269–5278.

Ye, J., Wang, C., Sumpter, R. Jr., Brown, M. S., Goldstein, J. L., and Gale, M. Jr. (2003). Disruption of hepatitis C virus RNA replication through inhibition of host protein geranylgeranylation. *Proc. Natl. Acad. Sci. U.S.A.* 100, 15865–15870.

Zhang, Z., and Zhang, R. (2008). Proteasome activator PA28 gamma regulates p53 by enhancing its MDM2-mediated degradation. *EMBO J.* 27, 852–864.

Zhong, J., Gastaminza, P., Cheng, G., Kapadia, S., Kato, T., Burton, D. R., Wieland, S. F., Uprichard, S. L., Wakita, T., and Chisari, F. V. (2005). Robust hepatitis C virus infection in vitro. *Proc. Natl. Acad. Sci. U.S.A.* 102, 9294–9299.

Conflict of Interest Statement: The authors declare that the research was conducted in the absence of any commercial or financial relationships that could be construed as a potential conflict of interest.

Received: 01 December 2011; accepted: 31 January 2012; published online: 14 February 2012.

Citation: Moriishi K and Matsuura Y (2012) Exploitation of lipid components by viral and host proteins for hepatitis C virus infection. Front. Microbio. 3:54. doi: 10.3389/fmicb.2012.00054

This article was submitted to Frontiers in Virology, a specialty of Frontiers in Microbiology.

Upregulation of nuclear PA28γ expression in cirrhosis and hepatocellular carcinoma

MOTOI KONDO[1], KOHJI MORIISHI[2], HIROSHI WADA[3], TAKEHIRO NODA[3], SHIGERU MARUBASHI[3], KENICHI WAKASA[4], YOSHIHARU MATSUURA[2], YUICHIRO DOKI[3], MASAKI MORI[3] and HIROAKI NAGANO[3]

[1]Evidence Based Medical Research Center, Osaka; [2]Department of Molecular Virology, Research Institute for Microbial Diseases, Osaka University, Osaka; [3]Department of Gastroenterological Surgery, Graduate School of Medicine, Osaka University, Osaka; [4]Department of Diagnostic Pathology, Graduate School of Medicine, Osaka City University, Osaka, Japan

Received September 16, 2011; Accepted December 2, 2011

DOI: 10.3892/etm.2011.415

Abstract. We previously reported that proteasome activator 28γ (PA28γ) is an oncogenic protein in hepatitis C virus (HCV) core protein transgenic mice. The aim of this study was to determine the role of PA28γ expression at the protein level in the development and progression of human hepatocarcinogenesis and hepatocellular carcinoma (HCC). Samples from tissues representing a wide spectrum of liver disease were analyzed, including histologically normal livers (n=5), HCV-related chronic hepatitis (CH) (n=15) and cirrhosis (n=31). The level of nuclear PA28γ increased with the progression of liver disease from CH to cirrhosis. The majority of cirrhotic livers (68%; 21/31) displayed high nuclear PA28γ expression. However, in half of the HCCs (50%; 18/36), little or no nuclear PA28γ expression was observed, while the remaining 50% (18/36) of the cases displayed high levels of nuclear PA28γ expression. A clinicopathological survey demonstrated a significant correlation between nuclear PA28γ expression and capsular invasion in HCC (P=0.026); a striking difference was found between nuclear PA28γ expression in non-tumor tissues and shorter disease-free survival (P<0.01). Moreover, nuclear PA28γ expression in non-tumor tissues correlated with the expression of molecules related to the genesis of hepatic steatosis and HCC, such as sterol regulatory element binding protein-1c mRNA. The findings suggest the involvement of nuclear PA28γ expression in the progression and relapse of HCC, and suggest that nuclear PA28γ is a potentially suitable target for the prevention and/or treatment of HCC.

Correspondence to: Dr Hiroaki Nagano, Department of Gastroenterological Surgery, Graduate School of Medicine, Osaka University, 2-2 Yamadaoka E-2, Suita, Osaka 565-0871, Japan
E-mail: hnagano@gesurg.med.osaka-u.ac.jp

Abbreviations: CH, chronic hepatitis; HBV, hepatitis B virus; HCC, hepatocellular carcinoma; HCV, hepatitis C virus; PA, proteasome activator; PBGD, porphobilinogen deaminase; RT-PCR, reverse transcription-polymerase chain reaction

Key words: proteasome activator 28γ, hepatocellular carcinoma, cirrhosis, western blotting, immunohistochemistry

Introduction

Hepatocellular carcinoma (HCC) is one of the most common malignancies worldwide, accounting for approximately 6% of all human carcinomas and 1 million deaths annually, with an estimated number of new cases of over 500,000/year (1). Clinical and experimental evidence suggests a link between infection with hepatitis C virus (HCV) and/or hepatitis B virus (HBV), chronic hepatitis (CH) and cirrhosis, as well as the progression of HCC. Liver cirrhosis is observed in up to 90% of patients with HCC, and HCV is the causative factor in 80% and HBV in 10% of cases in Japan (2-5). In the United States, almost 4 million individuals are infected with HCV each year which progresses to chronic hepatitis C, which could potentially progress to liver cirrhosis. The results are often liver failure or HCC. Chronic hepatitis C is the nation's leading cause of HCC, and according to the American Liver Foundation, is also the leading reason for liver transplantation. In Japan, HCV and/or HBV-based hepatitis and cirrhosis are also serious problems since they progress to HCC at a ratio of 5 to 7% per year (4,5). These findings strongly suggest the existence of a link between hepatocarcinogenesis and HCV/HBV infection and chronic liver inflammation.

Various therapies are currently in use for HCC. These include surgical resection, percutaneous ethanol injection (PEI), systemic or arterial chemotherapy using either single or combination drugs, transcatheter arterial chemoembolization (TACE), hormonal therapy and selective radiotherapy. However, the prognosis of patients with HCC remains poor, as they often develop intrahepatic and/or multicentric tumor recurrence, at a rate of 20-40% within 1 year, and ~80% within 5 years of therapy even when curative treatment is applied (6-9). Liver transplantation offers the best prognosis for patients with small HCC, although its use is limited due to the scarcity of donor organs. Therefore, an effective therapeutic strategy against HCC is required.

In a previous study, we reported that proteasome activator 28γ (PA28γ) directly enhances the degradation of the HCV core protein and plays a key role in the genesis of hepatic steatosis and HCC in HCV core protein transgenic mice (10). Furthermore, the above events were not observed in PA28γ-knockout mice. The present study is an extension of our previous study and was designed to assess the utility of PA28γ expression as a biological marker for HCV-related human liver disease and HCC. The findings showed the presence of high levels of nuclear PA28γ in multistep hepatocarcinogenesis and HCC invasion, suggesting that selective inhibitors of nuclear PA28γ may be useful in the prevention and/or treatment of this disease.

Materials and methods

Tissue samples. The study protocol was approved by the Human Ethics Review Committee of Osaka University, and a signed consent form was obtained from each subject for the use of tissue samples for medical research. Tissue samples were obtained from 51 patients with liver tumors, who underwent hepatectomy at the Department of Gastroenterological Surgery, Osaka University Hospital. All patients had HCV infection (28 patients) and some had HCV plus HBV infection (18 patients), but none had only HBV infection. The mean post-treatment follow-up period was 6.2±2.5 years ± standard deviation (SD). The excised hepatic tissue samples were examined immunohistochemically for PA28γ expression, including 46 paired HCCs. Non-tumor tissues were also examined, which comprised 15 CH-based livers (5 chronic active hepatitis and 10 chronic inactive hepatitis) and 31 cirrhotic livers. Prior to hepatectomy for HCC, 10 patients were treated with transarterial embolization (TAE). In these cases, histopathological examination showed complete hepatic necrosis. Histologically normal livers were also obtained from patients negative for hepatic viral infections who had liver metastasis secondary to colorectal cancer.

For immunohistochemistry, the tissue samples were fixed in 10% neutral buffered formalin, processed through graded ethanol and embedded in paraffin. The samples were frozen immediately in liquid nitrogen and stored at -80°C for subsequent analysis by reverse transcription-polymerase chain reaction (RT-PCR).

Histopathological examination. Tissue sections (4 μm thick) were deparaffinized in xylene, rehydrated and stained with hematoxylin and eosin solution. Separation of the tissues into non-tumor and tumor tissues was determined by a pathologist (K.W.) who was blinded to the clinical background. For non-tumor tissues, the presence of inflammation or cirrhotic nodules was examined. Tumor tissues were examined for the following characteristics: cell differentiation (well, moderate, poorly differentiated), number of tumors, capsular formation, septal formation, capsular invasion, portal vein tumor thrombus formation and hepatic vein invasion.

Preparation of anti-human PA28γ antibody. Chicken anti-human PA28γ antibody was prepared by immunization using the synthetic peptides of residues from 75 to 88, SHDGLDGPTYKKRR, of human PA28γ. The antibody was purified by affinity chromatography using beads conjugated with the antigen peptide.

Immunohistochemistry and evaluation of PA28γ immunostaining. Formalin-fixed tissues were embedded in paraffin according to the standard procedures. For immunohistochemistry, formalin-fixed tissue sections were boiled in Target Retrieval Solution (Dako, Glostrup, Denmark) and then treated with 3% H_2O_2. The activated sections were washed twice with phosphate-buffered saline (PBS), blocked with PBS containing 5% bovine serum albumin, and incubated overnight with the purified chicken antibody to PA28γ, followed by incubation with horseradish peroxidase-conjugated anti-chicken IgG antibody (ICN, Biomedicals, Inc., Aurora, OH, USA) as a secondary antibody. Immunoreactive antigen was visualized with 3,3'-diaminobenzidine substrate. The resulting sections were counterstained with hematoxylin. Staining of endogenous PA28γ with the antibody was identified in normal mouse liver sections but not in the liver sections from PA28γ-deficient mice. Pre-immune purified antibody did not react with any other antigen in these sections under the experimental conditions.

For evaluation of PA28γ immunostaining, each section was scored for nuclear and cytoplasmic staining using a scale from 0 to 2 where 0 represented negative or faint staining, 1 represented moderate staining, and 2 represented strong staining. In general, the nuclei of the bile ducts faintly expressed PA28γ (Fig. 1a). Thus, the staining level was used as a nuclear inner control within the sample, which was designated arbitrarily as intensity level 0. Also, slightly higher expression was designated arbitrarily as intensity level 1 and clearly higher expression was designated arbitrarily as intensity level 2. PA28γ expression was very faint or undetectable in the vascular epithelia and nuclei (Fig. 1a), whereas the cytoplasm of bile duct epithelial cells and nuclei devoid of significant inflammation generally expressed faint levels of PA28γ (Fig. 1a). For semi-quantitative analysis, the latter level of staining was used as a cytoplasmic inner control within the sample, and designated arbitrarily as intensity level 0. Furthermore, a slightly higher expression was designated arbitrarily as intensity level 1 whereas clearly higher expression was designated arbitrarily as intensity level 2. PA28γ expression was generally heterogeneous in each sample. For assessment of nuclear and cytoplasmic PA28γ, 4 high-power fields in each specimen were selected at random, and staining was examined under high power magnification. More than 1,000 cells were counted to determine the labeling index, which represented the percentage of immunostained cells relative to the total number of cells. The tissue samples were also categorized as positive (levels 1 and 2) and negative (level 0) for evaluation of the relationship between immunostaining and various clinicopathological factors.

Semi-quantitative RT-PCR. RNA extraction was carried out with TRIzol reagent using the single-step method, and the cDNA was generated with avian myeloblastosis virus reverse transcriptase (Promega, Madison, WI, USA), as described previously (11). Sterol regulatory element binding protein-1c (SREBP-1c) mRNA expression was analyzed semi-quantitatively using the multiplex RT-PCR method. In this assay, the

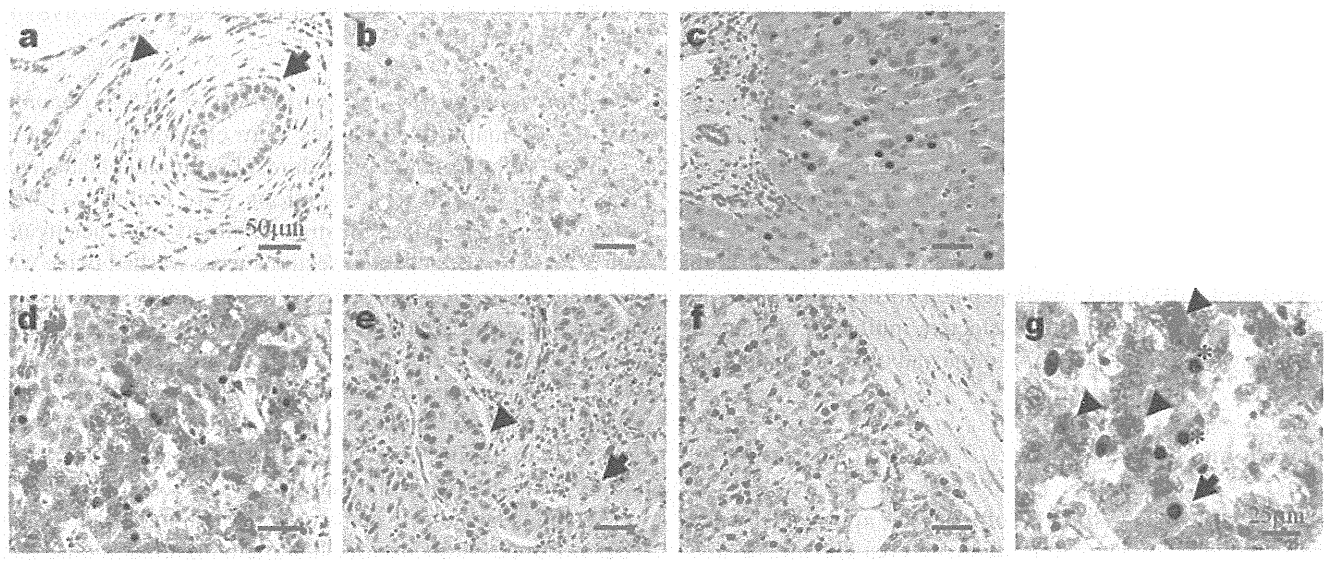

Figure 1. Immunohistochemical staining for PA28γ. (a-f) Representative samples for bile duct (inner control), vascular epithelium and various liver pathologies; (a) bile duct (arrow), vascular epithelium (arrowhead); (b) normal liver; (c) chronic hepatitis; (d) cirrhotic liver; (e) HCC with high nuclear PA28γ expression (arrowhead; left side) and non-tumor liver tissue with low nuclear PA28γ expression (arrow; right side); (f) HCC with low expression of nuclear PA28γ. Magnification, x200. (g) High-power view of liver section shown in (d). Note the faint staining of hepatocytes with high expression of nuclear PA28γ (arrow; hepatocytes, level 0 and nucleus, level 2), moderate staining of hepatocytes with high expression of nuclear PA28γ (asterisk; hepatocyte, level 1 and nucleus, level 2) and strong staining of hepatocytes with low expression of nuclear PA28γ (arrowhead; hepatocyte, level 2 and nucleus, level 0). Magnification, x400. No staining was observed when the primary antibody was substituted by non-immunized rabbit IgG or TBS (data not shown). PA28γ, proteasome activator 28γ; HCC, hepatocellular carcinoma; IgG, immunoglobulin G; TBS, Tris-buffered saline.

housekeeping gene, porphobilinogen deaminase (PBGD), was used as the internal control. This gene is favored over β-actin or glyceraldehyde-3-phosphate dehydrogenase as a reference gene for competitive PCR amplification as the presence of pseudogenes for the latter housekeeping genes may produce false-positive signals from genomic DNA contamination (12,13). In addition, in order to minimize possible inter-PCR differences, PCR was performed with SREBP-1c and PBGD primers in an identical tube, under unsaturated conditions. PCR was performed in a 25-μl reaction mixture containing 1 μl of the cDNA template, 1X Perkin-Elmer PCR buffer, 1.5 mM $MgCl_2$, 0.8 mM deoxynucleotide triphosphates, 0.8 μM of each primer for SREBP-1c and 80 nM PBGD, and 1 unit of TaqDNA polymerase (AmpliTaq Gold; Roche Molecular Systems, Inc.). The PCR primers used for the detection of SREBP-1c and PBGD cDNAs were synthesized as described previously (14,15). The conditions for multiplex PCR were one cycle of denaturation at 95˚C for 12 min, followed by 40 cycles at 95˚C for 1 min, 62˚C for 1 min and 72˚C for 1 min, and a final extension at 72˚C for 10 min. The electrophoresed PCR products were scanned by densitometry, and the relative value of the SREBP-1c band relative to that of PBGD was calculated for each sample.

Statistical analysis. Data were expressed as the means ± SD. The Chi-square test and Fisher's exact probability test, or the log-rank test, were used to examine the association between PA28γ expression and the clinicopathological parameters or prognosis. A P-value of <0.05 was considered to indicate a statistically significant difference. Statistical analysis was performed using the StatView-J-5.0 program (SAS Institute, Cary, NC, USA).

Results

Immunohistochemical analysis of PA28γ. Immunohistochemical assays were performed on a series of 46 paired HCCs and their matched non-tumor tissues, and 5 normal livers. The labeling index of nuclear PA28γ showed a wide spectrum and increased from low in the normal livers to strong in the cirrhotic livers (Fig. 1b-d). Specifically, the nuclear PA28γ labeling index was generally low in the normal liver tissues, but was moderate-strong in HCV-related liver tissues. The nuclear labeling index was markedly higher in the majority of cirrhotic liver tissues. Fig. 2 summarizes the above results and the analysis of cytoplasmic expression of PA28γ. The difference in the PA28γ-nuclear labeling index between normal and cirrhotic livers was significant (P<0.0001) as was that between CH and cirrhosis (P<0.0001) (Fig. 2A). Also, the difference in the proportion of the PA28γ-cytoplasmic expression labeling index between normal and cirrhotic livers was significant (P<0.05) (Fig. 2B). The mean labeling indexes of nuclear PA28γ expression was 42% in both HCC and HCV-related livers.

To evaluate the relationship between immunohistochemical staining and various clinicopathological factors, we divided the samples into nuclear PA28γ high index (≥42%) and low index (<42%) groups. The labeling index was low in half of the examined HCC cases (50%; 18/36) and markedly high in the other half (50%; 18/36) (Table I). The labeling index was low in 30% (14/46) of HCV-related cases and markedly higher in the remaining 70% (32/46) (Table II). The samples were also divided into 2 groups according to the labeling index of cytoplasmic staining. The mean PA28γ-labeling index of the HCC and HCV-related cases was 58 and 80%, respectively. The labeling index was low in 47% (17/36) and high in 53% (19/36)

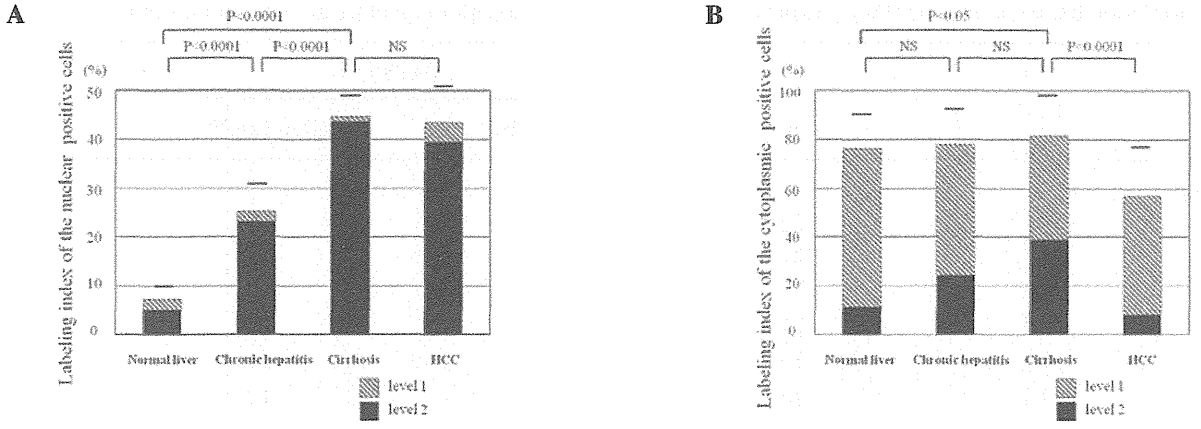

Figure 2. (A) Nuclear PA28γ expression in multistep hepatocarcinogenesis. The labeling index increased in a stepwise manner with the severity of liver damage and carcinogenesis. Quantitative analysis showed that 25, 10 and 1% of cells of the normal liver, CH and cirrhosis, respectively, were moderately positive (level 1). In HCCs, 10% of cells were evaluated as moderately positive (level 1). (B) Cytoplasmic PA28γ expression in multistep hepatocarcinogenesis. The expression increased slightly in a stepwise manner. Quantitative analysis showed that 80, 68 and 50% of cells of the normal liver, CH and cirrhosis, respectively, were moderately positive (level 1). In HCCs, 82% of cells were evaluated as moderately positive (level 1). PA28γ, proteasome activator 28γ; CH, chronic hepatitis; HCC, hepatocellular carcinoma. NS, not significant.

Table I. Correlation between nuclear PA28γ expression and various clinicopathological parameters in patients with HCC.

		PA28γ		
	n	Low (<42%)	High (≥42%)	P-value
Age (years)				
≥60	15	7	8	
<60	21	11	10	NS
Gender				
Male	21	10	11	
Female	15	8	7	NS
Tumor size				
≤2 cm	8	4	4	
>2 cm	28	14	14	NS
Histological type				
Well/moderately differentiated	5	2	3	
Poorly differentiated	31	16	15	NS
Hepatic vein invasion				
Yes	6	2	4	
No	30	16	14	NS
Portal vein tumor thrombus				
Yes	5	2	3	
No	31	16	15	NS
Number of tumors				
Multiple[a]	3	1	2	
Solitary	33	17	16	NS
Septum formation				
Yes	15	8	7	
No	21	10	11	NS
Capsular formation				
Yes	14	6	8	
No	22	12	10	NS
Capsular invasion				
Yes	8	1	7	
No	6	5	1	0.026

[a]This category includes intrahepatic metastasis and multicentric carcinogenesis. PA28γ, proteasome activator 28γ; HCC, hepatocellular carcinoma; NS, not significant.

Table II. Correlation between nuclear PA28γ expression and various clinicopathological parameters in non-tumor liver tissues.

		PA28γ		
	n	Low (<42%)	High (≥42%)	P-value
Age (years)				
≥60	22	5	17	
<60	24	9	15	NS
Gender				
Male	27	6	21	
Female	19	8	11	NS
HCV	28	9	19	
HBV	0			
HCV plus HBV	18	5	13	NS
Inflammatory status (HAI score)				
Absent-mild (0-3)	22	12	10	
Moderate-severe (>4)	24	2	22	0.0007
Degree of fibrosis (HAI score)				
Absent-moderate (0-2)	12	11	1	
Severe-cirrhosis (>3)	34	3	31	<0.0001

NS, not significant; PA28γ, proteasome activator 28γ; HCV, hepatitis C virus; HBV, hepatitis B virus; HAI, histological activity index.

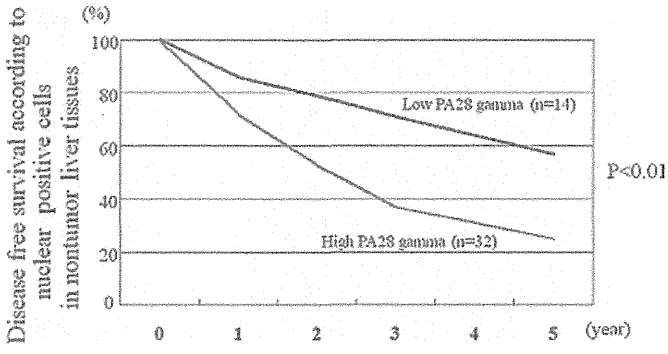

Figure 3. Disease-free survival based on nuclear PA28γ expression in non-tumor tissues. The disease-free survival was significantly different between patients with high nuclear PA28γ expression (levels 1 and 2) and those with low nuclear PA28γ expression (level 0) (P<0.01). PA28γ, proteasome activator 28γ.

of the HCC cases. The respective values for HCV-related cases were 28% (13/46) and 72% (33/46). All cut-off values used were according to the mean labeling index.

Correlation between nuclear PA28γ expression and clinicopathological parameters. We examined the correlation between PA28γ nuclear expression analyzed in 36 HCCs (10 samples with complete necrosis by TAE were excluded from this analysis) and various clinicopathological features (Table I). The cases were divided into two groups based on the labeling index of nuclear expression of PA28γ, using a cut-off mean value of 42%. There was a significant difference in PA28γ expression based on capsular invasion (Table I). We also analyzed the relationship between nuclear PA28γ expression in non-tumor tissues (15 CH and 31 cirrhosis) and disease-free survival, as the pathologic status of non-tumor tissues has been shown to correlate with the relapse of HCC (16-18). The disease-free survival, but not overall survival (P=0.052), was significantly different between high and low nuclear PA28γ expressors (P<0.01) (Fig. 3). In addition, PA28γ expression in non-tumor tissues correlated closely with active inflammation and fibrosis (Table II).

In univariate analysis, PA28γ expression in non-tumor liver tissues, portal vein tumor thrombus, inflammatory status and degree of fibrosis in the non-cancerous liver tissue were significant factors for disease-free survival. These variables were subsequently entered into multivariate analysis. The results identified nuclear PA28γ expression level [95% confidence interval (CI), 1.82-3.22; P<0.01], portal vein tumor thrombus (95% CI, 1.33-6.38; P=0.023), inflammatory status (95% CI, 2.11-3.58; P=0.012) and degree of fibrosis (95% CI, 1.99-7.21; P<0.01) as independent factors for disease-free survival (Table III).

SREBP-1c expression. Five CH and five cirrhotic liver tissues were selected to analyze the correlation between nuclear PA28γ expression and SREBP-1c gene expression in non-tumor liver tissues. Fig. 4 shows a clear correlation between nuclear PA28γ expression and SREBP-1c gene expression.

Discussion

The present study shows that non-tumor liver tissues commonly express high levels of nuclear PA28γ protein relative to those of carcinoma tissues. These results are contradictory to those from other studies on other types of cancer, such as thyroid carcinoma; the nuclear PA28γ level was higher in these tumors compared to non-tumor tissues (19). While the exact reason for

Table III. Multivariate analysis of clinicopathological factors for disease-free survival in patients with HCC.

	n	Relative risk	95% confidence interval	P-value
PA28γ				
High	32	2.67	1.82-3.22	<0.01
Low	14			
Portal vein tumor thrombus				
Yes	5	2.21	1.33-6.38	0.023
No	31			
Inflammatory status (HAI score)				
Absent-mild (0-3)	22	2.59	2.11-3.58	0.012
Moderate-severe (>4)	24			
Degree of fibrosis (HAI score)				
Absent-moderate (0-2)	12	2.68	1.99-7.21	<0.01
Severe-cirrhosis (>3)	34			

HCC, hepatocellular carcinoma; PA28γ, proteasome activator 28γ; HAI, histological activity index.

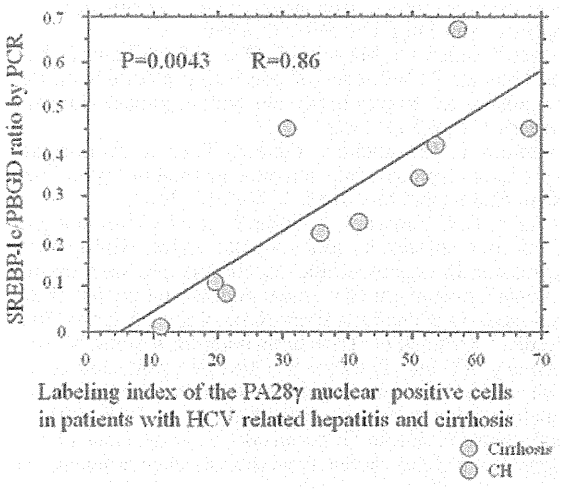

Figure 4. Linear correlation analysis of nuclear PA28γ expression and SREBP-1c gene expression in patients with cirrhosis and chronic hepatitis (CH) (P=0.0043). PA28γ, proteasome activator 28γ; HCV, hepatitis C virus. SREBP-1c, sterol regulatory element binding protein-1c.

the different results is not known at present, it is likely to be related to the type of control tissue used in the present study; the non-tumor tissues were mostly not normal, consisting of HCV-infected CH or cirrhotic tissues. In support of this conclusion, normal liver tissues from patients with metastatic liver tumors from patients with colorectal carcinoma who were negative for HCV/HBV showed low expression of nuclear PA28γ.

In non-neoplastic liver tissues, we found a wide spectrum of nuclear PA28γ expression from normal liver to cirrhosis. Our results also show that active inflammation with hepatitis virus induces nuclear PA28γ in CH and cirrhotic livers (Table II). This is reasonable considering the fundamental action of nuclear PA28γ as a mediator of inflammation. Another mechanism for the high induction of nuclear PA28γ in cirrhosis might be related to the degradation of the HCV core protein by PA28γ and its translocation from the cytoplasm to the nucleus, based on the results of our previous study (10). In fact, nuclear PA28γ-expressing cells had no or faint-to-moderate cytoplasmic PA28γ expression (Fig. 1c and g). Furthermore, the nuclear overexpression could be due to the relatively hypoxic microenvironment in the cirrhotic liver. In this regard, we hypothesized that hypoxia might directly induce PA28γ, which in turn enhances angiogenesis via the enhanced release of a battery of angiogenic growth factors, such as vascular endothelial growth factor (VEGF). Since the VEGF level is increased in cirrhosis (20), it is possible that nuclear PA28γ may improve the ischemic/hypoxic microenvironment in the cirrhotic liver through upregulation of angiogenesis. Although cirrhotic nodules occasionally show p53 mutation and increased telomerase activity (21,22), cirrhosis is not considered a premalignant lesion. However, it is apparent from a number of etiological studies that cirrhosis is a strong risk factor for HCC. In this context, nuclear PA28γ expression in cirrhosis might be a prerequisite for the genesis of premalignant dysplastic nodules or early cancer.

From a clinical point of view, it is interesting to note the correlation between high nuclear PA28γ expression in non-tumor tissues and the relapse of HCC. The prognosis of HCC is generally unfavorable. Although primary tumors are curatively resected, 50-60% of patients develop relapse within 5 years. This is due to either a newly established tumor from the remnant liver, a process termed multicentric carcinogenesis, or recurrence of the original tumor. One possible mechanism for a link between nuclear PA28γ and disease relapse is that high expression of PA28γ in the remnant liver may contribute to carcinogenesis. Nuclear PA28γ expression highly correlated with the presence of active inflammation (P<0.0001). Furthermore, active inflammation in non-tumor tissues has been reported to be associated with relapse of HCC (17,23,24).

In the present study, a clinicopathological survey demonstrated a significant correlation between nuclear PA28γ protein expression and capsular invasion of the cancer tissue. This

finding is in agreement with a recent study that showed increased expression of PA28γ protein during cancer progression and its correlation with PCNA labeling index (19). Thus, the results suggest the possible involvement of PA28γ in HCC progression. Further studies of larger population samples are required to confirm the clinical significance of nuclear PA28γ in HCC. This is particularly important, as the overall survival of patients with high nuclear PA28γ expression was worse than that of those with low expression level (P=0.052) (data not shown).

Also in our series, the labeling index of cytoplasmic expression of PA28γ significantly increased from normal liver to cirrhotic liver (Fig. 2b). Further extended studies are required to determine the importance of cytoplasmic expression of PA28γ in HCC and HCV-related liver.

In conclusion, the present study demonstrates a close correlation between nuclear PA28γ expression in liver tissue and the development and progression of HCC, as well as its possible involvement in HCC relapse. Further studies are required to examine the therapeutic benefits of the suppression of nuclear PA28γ expression in HCV-related CH, cirrhosis or HCC.

References

1. Montalto G, Cervello M, Giannitrapani L, Dantona F, Terranova A and Castagnetta LA: Epidemiology, risk factors, and natural history of hepatocellular carcinoma. Ann NY Acad Sci 963: 13-20, 2002.
2. Okuda K: Hepatocellular carcinoma: Recent progress. Hepatology 15: 948-963, 1992.
3. Kew MC and Popper H: Relationship between hepatocellular carcinoma and cirrhosis. Semin Liver Dis 4: 136-146, 1984.
4. Ikeda K, Saitoh S, Koida I, Arase Y, Tsubota A, Chayama K, Kumada H and Kawanishi M. A multivariate analysis of risk factors for hepatocellular carcinogenesis: A prospective observation of 795 patients with viral and alcoholic cirrhosis. Hepatology 18: 47-53, 1993.
5. Shiratori Y, Shiina S, Imamura M, *et al*: Characteristic difference of hepatocellular carcinoma between hepatitis B- and C- viral infection in Japan. Hepatology 22: 1027-1033, 1995.
6. Nagasue N, Uchida M, Makino Y, *et al*: Incidence and factors associated with intrahepatic recurrence following resection of hepatocellular carcinoma. Gastroenterology 105: 488-494, 1993.
7. Ikeda K, Saitoh S, Tsubota A, Arase Y, Chayama K, Kumada H, Watanabe G and Tsurumaru M: Risk factors for tumor recurrence and prognosis after curative resection of hepatocellular carcinoma. Cancer 71: 19-25, 1993.
8. Shimada M, Takenaka K, Gion T, *et al*: Prognosis of recurrent hepatocellular carcinoma: a 10-year surgical experience in Japan. Gastroenterology 111: 720-726, 1996.
9. Kumada T, Nakano S, Takeda I, *et al*: Patterns of recurrence after initial treatment in patients with small hepatocellular carcinoma. Hepatology 25: 87-92, 1997.
10. Moriishi K, Mochizuki R, Moriya K, *et al*: Critical role of PA28gamma in hepatitis C virus-associated steatogenesis and hepatocarcinogenesis. Proc Natl Acad Sci USA 104: 1661-1666, 2007.
11. Myers J, Mehta P, Hunter AW, Bernstein SA and Erickson PA. Automated double-label immunohistochemistry. J Surg Pathol 1: 105-113, 1995.
12. Chretien S, Dubart A, Beaupain D, *et al*: Alternative transcription and splicing of the human porphobilinogen deaminase gene result either in tissue-specific or in housekeeping expression. Proc Natl Acad Sci USA 85: 6-10, 1988.
13. Nagel S, Schmidt M, Thiede C, Huhn D and Neubauer A: Quantification of Bcr-Abl transcripts in chronic myelogenous leukemia (CML) using standardized, internally controlled, competitive differential PCR (CD-PCR). Nucleic Acids Res 24: 4102-4103, 1996.
14. Kim KH, Hong SP, Kim K, Park MJ, Kim KJ and Cheong J: HCV core protein induces hepatic lipid accumulation by activating SREBP1 and PPARgamma. Biochem Biophys Res Commun 355: 883-888, 2007.
15. Finke J, Fritzen R, Ternes P, Lange W and Dolken G: An improved strategy and a useful housekeeping gene for RNA analysis from formalin-fixed, paraffin-embedded tissues by PCR. Biotechniques 14: 448-453, 1993.
16. Sasaki Y, Imaoka S, Fujita M, *et al*: Regional therapy in the management of intrahepatic recurrence after surgery for hepatoma. Ann Surg. 206: 40-47, 2007.
17. Ko S, Nakajima Y, Kanehiro H, *et al*: Significant influence of accompanying chronic hepatitis status on recurrence of hepatocellular carcinoma after hepatectomy. Result of multivariate analysis. Ann Surg 224: 591-595, 1996.
18. Sasaki Y, Imaoka S, Masutani S, Ohashi I, Ishikawa O, Koyama H and Iwanaga T: Influence of coexisting cirrhosis on long-term prognosis after surgery in patients with hepatocellular carcinoma. Surgery 112: 515-21, 1992.
19. Okamura T, Taniguchi S, Ohkura T, *et al*: Abnormally high expression of proteasome activator-gamma in thyroid neoplasm. J Clin Endocrinol Metab 88: 1374-1383, 2003.
20. El-Assal ON, Yamanoi A, Soda Y, *et al*: Clinical significance of microvessel density and vascular endothelial growth factor expression in hepatocellular carcinoma and surrounding liver: possible involvement of vascular endothelial growth factor in the angiogenesis of cirrhotic liver. Hepatology 27: 1554-1562, 1998.
21. Raedle J, Oremek G, Truschnowitsch M, Lorenz M, Roth WK, Caspary WF and Zeuzem S: Clinical evaluation of autoantibodies to p53 protein in patients with chronic liver disease and hepatocellular carcinoma. Eur J Cancer 34: 1198-1203, 1998.
22. Kishimoto Y, Shiota G, Kamisaki Y, *et al*: Loss of the tumor suppressor p53 gene at the liver cirrhosis stage in Japanese patients with hepatocellular carcinoma. Oncology 54: 304-310, 1997.
23. Tarao K, Takemiya S, Tamai S, *et al*: Relationship between the recurrence of hepatocellular carcinoma (HCC) and serum alanine aminotransferase levels in hepatectomized patients with hepatitis C virus-associated cirrhosis and HCC. Cancer 79: 688-694, 1997.
24. Ko S, Nakajima Y, Kanehiro H, *et al*: Influence of associated viral hepatitis status on recurrence of hepatocellular carcinoma after hepatectomy. World J Surg 21: 1082-1086, 1996.

SCIENTIFIC REPORTS

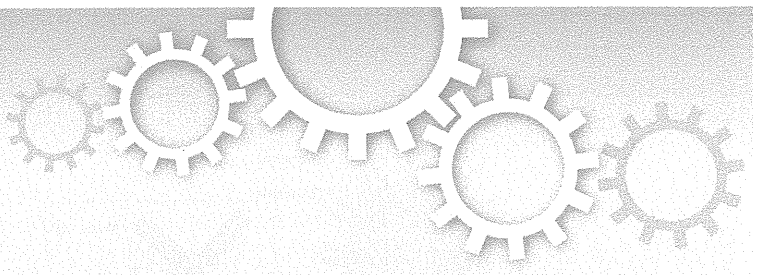

OPEN

SUBJECT AREAS:
NANOBIOTECHNOLOGY
SENSORS
NANOPARTICLES
SURFACE PATTERNING

Received
21 August 2012

Accepted
10 October 2012

Published
9 November 2012

Correspondence and requests for materials should be addressed to S.K. (skuroda@agr.nagoya-u.ac.jp)

Nano-visualization of oriented-immobilized IgGs on immunosensors by high-speed atomic force microscopy

Masumi Iijima, Masaharu Somiya, Nobuo Yoshimoto, Tomoaki Niimi & Shun'ichi Kuroda

Graduate School of Bioagricultural Sciences, Nagoya University, Nagoya, Aichi 464-8601, Japan.

Oriented immobilization of sensing molecules on solid phases is an important issue in biosensing. In case of immunosensors, it is essential to scrutinize not only the direction and shape of immunoglobulin G (IgG) in solution but also the real-time movement of IgGs, which cannot be achieved by conventional techniques. Recently, we developed bio-nanocapsules (BNCs) displaying a tandem form of the IgG Fc-binding Z domain derived from *Staphylococcus aureus* protein A (ZZ-BNC) to enhance the sensitivity and antigen-binding capacity of IgG *via* oriented-immobilization. Here, we used high-speed atomic force microscopy (HS-AFM) to reveal the fine surface structure of ZZ-BNC and observe the movement of mouse IgG3 molecules tethered onto ZZ-BNC in solution. ZZ-BNC was shown to act as a scaffold for oriented immobilization of IgG, enabling its Fv regions to undergo rotational Brownian motion. Thus, HS-AFM could decipher real-time movement of sensing molecules on biosensors at the single molecule level.

Due to the high specificity and affinity of biological molecules (*e.g.* immunoglobulin G (IgG), ligands, receptors, aptamers, sugar chains, lectins), biosensors are expected to be a promising technology for sensing various biological materials. The sensor surface (*e.g.*, glass or metal) is commonly functionalized with chemical crosslinking or self-assembled monolayers (SAMs)[1]. Especially, long-chain (number of methylene groups $n > 10$) alkanethiols assemble in a crystalline-like way and can introduce uniform functional groups onto gold surface. While biological molecules were subsequently immobilized on the sensor surface, the control over the orientation of these molecules (*i.e.*, oriented-immobilization of IgGs)[2] has not so far been fully achieved. In case of immunosensors, the crosslinking molecules should neither increase steric hindrance around the antigen-recognition Fv regions nor reduce the antigen-recognition activity of IgGs and, furthermore, should align the Fv regions for efficient antigen-recognition. Specific sites within IgG molecules have been used to achieve oriented immobilization, such as the Fc region *via* an Fc-binding protein A or G[3,4], aldehyde groups introduced into the carbohydrate moiety of the C_H2 domain *via* an hydrazide-containing crosslinker[5], and the thiol group of monovalent Fab' fragments *via* a thiol-containing solid phase[6]. However, the orientation of protein A or G itself cannot be fully controlled on the solid phase. Chemical and enzymatic treatments may affect the antigen-recognition activity of IgGs. These situations led us to develop rigid and self-assembled scaffolds for aligning IgGs at the nanoscale level, without modification.

We previously developed ZZ-BNCs of ~30 nm diameter by expressing the gene encoding hepatitis B virus (HBV) surface antigen (HBsAg) L protein with a tandem form of Fc-binding Z domain (Fig. 1a)[7] in yeast[8]. ZZ-BNC contains about 120 molecules of ZZ-L protein (N-terminally ZZ-fused L protein) embedded in a liposome and has ability for capturing ~60 mouse IgG molecules, as well as displaying all the IgG Fv regions outwardly[9]. Furthermore, ZZ-BNCs can enhance the sensitivity of immunosensors[9] and immunoassays[10,11] not only through the oriented immobilization of antibodies but also the clustering of antibodies and labelling molecules. Thus, ZZ-BNC is a promising scaffold for a variety of conventional immunosensors and immunoassays.

To evaluate immunosensors, it is necessary to elucidate not only the direction and shape of IgGs on the solid phase in solution but also the real-time movement of IgGs. However, conventional techniques cannot fully analyze the real-time movement of IgGs[12–14]. Particularly, it is difficult for AFM to distinguish IgGs from surrounding molecules using these static observations (snapshots). Recently, HS-AFM (high-speed atomic force microscopy) equipped with a highly sensitive, ultra-fast cantilever and efficient AFM scanning capabilities, have

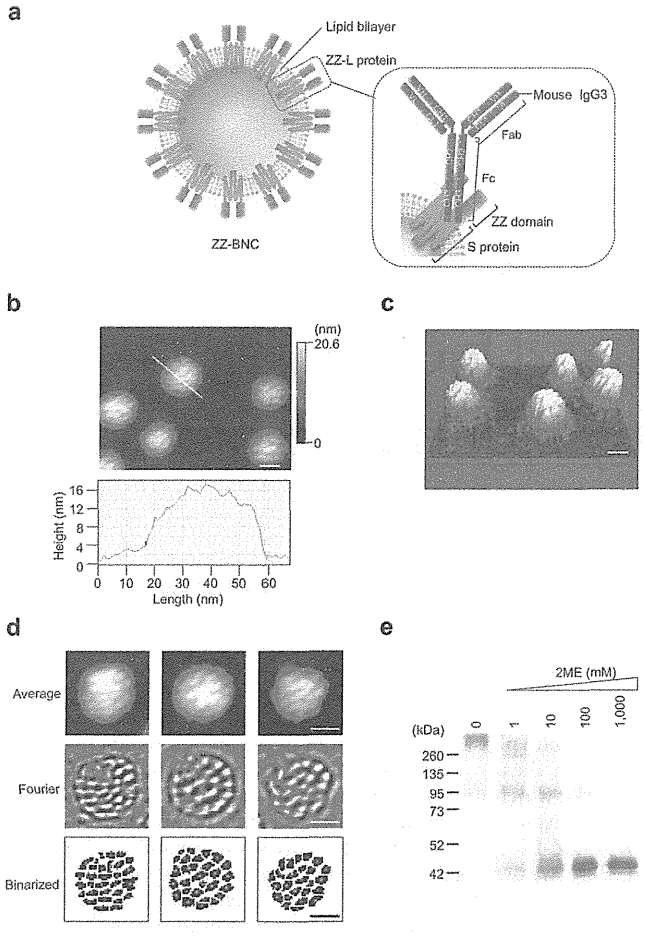

Figure 1 | HS-AFM analyses of ZZ-BNC in solution. (a) Structure of ZZ-BNC. One ZZ-BNC particle consists of about 120 ZZ-L proteins embedded in a lipid bilayer. The dimeric forms of ZZ-L proteins are described in this study. Mouse IgG3 could interact with the ZZ domain through domain B between C_H2 and C_H3 of the Fc subunit[32]. (b) (upper), (c) HS-AFM images of ZZ-BNCs in 2D and 3D, respectively. Bars, 20 nm. The surface morphology of ZZ-BNC is shown in (b) (bottom). (d) Single-particle reconstructions of ZZ-BNC by EMAN software, line 1; average images, line 2; Fourier transformed images, line 3; binarized images. (e) SDS-PAGE analyses of ZZ-BNC reduced with 0–1,000 mM 2ME (0.5 μg protein/lane), followed by silver staining.

demonstrated biomolecule dynamics in solution[15], encouraging us to analyze the behaviour of IgGs in solution for rigorous evaluation of immunosensors. Furthermore, the surface analysis using HS-AFM could contribute to the refinement not only of immunosensors but also of a variety of biosensors.

Results

Elucidation of fine surface structure of ZZ-BNC in solution. When analyzed a topological image of ZZ-BNCs on a mica surface by HS-AFM, they showed nanoparticles with rough surfaces (51.7 ± 4.8 nm in diameter; 17.6 ± 1.0 nm in height (mean ± SD, n = 19)) (Fig. 1b and c). The volume and surface area of an average ZZ-BNC were calculated to be 21,300 nm^3 and 5,170 nm^2, respectively, corresponding to those of a spherical ~40.6-nm particle. Because this value agreed well with the diameter obtained by dynamic light scattering (45.4 ± 2.2 nm), ZZ-BNCs were considered to adsorb onto mica surface without disrupting their capsule structure. Semi-automated, single-particle reconstructions using the EMAN software[16] (10 particles from 48 frames) revealed protrusions on the surface of ZZ-BNC (Fig. 1d). The number and area of protrusions were estimated by ImageJ software to be 27 ± 3 and 28.9 ± 10.1 nm^2, respectively. The diameter was 6.1 ± 3.6 nm. The distance between adjacent protrusions (centre to centre) was 8.2 ± 1.7 nm, which agrees well with the space (~6 nm) between two HBsAg proteins on the HBV virion[17]. One ZZ-BNC was estimated to possess 54 protrusions, while reported to contain about 120 molecules of ZZ-L protein[9]. Meanwhile, the HBsAg protein of the HBV virion[18], as well as the HBsAg L protein of BNC[8], is a transmembrane protein containing three membrane-spanning domains as dimeric[19] and multimeric[8] forms. ZZ-BNCs were then reduced with 0–1,000 mM 2-mercaptoethanol (2ME), separated by SDS-PAGE, and stained with silver (Fig. 1e). By increasing the concentration of 2ME, two major bands of 96 and >260 kDa were gradually shifted to 96 and 48 kDa, and finally converged to 48 kDa, strongly suggesting that nascent ZZ-L proteins form a dimer by intramolecular disulfide bonds which then form multimers by intermolecular disulfide bonds, as previously proposed for recombinant mammalian cell-derived HBsAg L protein[20]. Taken together, each protrusion on ZZ-BNCs may be a ZZ-L dimer containing six membrane-spanning domains, which is corroborated by the fact that the diameter of the protrusions (6.1 ± 3.6 nm) is consistent with that of seven membrane-spanning rhodopsin (~4.3 nm)[21].

Observation of mouse IgG3 in solution. We next observed mouse IgG3 molecules in solution by HS-AFM (Fig. 2a). Conventional AFM observation of IgG molecules on a mica surface in air have shown that the hinge region of IgG is flexible, allowing two Fab subunits to rotate about their axes to present the side to the mica surface, with deposition of the Fc subunit on the opposite side in two forms (extended and folded)[22]. Assuming that the vertical length of Fab subunits is consistent amongst IgG forms, each IgG was identified as a Y-shaped structure including three subunits (two Fab and one Fc) in extended or folded form. By measuring the size of the extended form of IgG (n = 3), the distance between the two Fab subunits was calculated at 26.8 ± 2.4 nm, and those between the Fc subunit and each Fab subunit at 32.5 ± 5.7 nm and 31.0 ± 6.3 nm, respectively. The width of the Fc subunit was 8.9 ± 1.6 nm. The greatest height of mouse IgG3 was 3.7 ± 0.5 nm and the centre of mass was estimated to be located at 19.1 ± 4.0 nm from the tip of the Fc subunit. These sizes of mouse IgG3 molecules are consistent with those of various IgG measurements obtained by conventional AFM observations[23]. We previously reported that one ZZ-BNC can capture a maximum of 60 IgG molecules[9]. When the surface of ZZ-BNC (5,170 nm^2; radius, 20.3 nm) was filled with Fc subunits (base area, 32.8 ± 6.0 nm^2; height, 19.1 ± 4.0 nm) in close-packed arrangement, ZZ-BNC could be surrounded by 161 ± 29 molecules of Fc subunits. On the other hand, ZZ-BNC fully covered with Fc subunits (surface area, 19,500 nm^2; radius, 39.4 nm) could be surrounded by 197 ± 18 molecules of $F(ab')_2$ subunits (base area, 99.3 ± 8.8 nm^2; height, 9.6 ± 2.0 nm), suggesting that Fc subunits on ZZ-BNC contact one another intermolecularly, rather than $F(ab')_2$ subunits. Consequently, each IgG could be tethered onto the surface of ZZ-BNC at appropriate intervals, thereby improving antigen recognition by the Fv region.

Real-time movement of mouse IgG3 on ZZ-BNC in solution. For developing the next generation of immunosensors, it is a prerequisite to analyze and optimize the real-time movement of immobilized IgGs in solution at the single molecular level. ZZ-BNCs adsorbed onto gold surfaces were immersed into PBS (0 s), contacted with mouse IgG3 (55 s, yellow arrows in Figs. 2b and d), and then subjected to time-lapse imaging with HS-AFM (0.2 frames per second (fps), total 1,300 s, 260 frames (Fig. 2b and Supplementary Movie 1). After 45 s from the addition of IgG (100 s from the start), some of the ZZ-BNCs exhibited a rough surface. After 95 s from the addition of IgG (150 s from the start), the height of three ZZ-BNCs

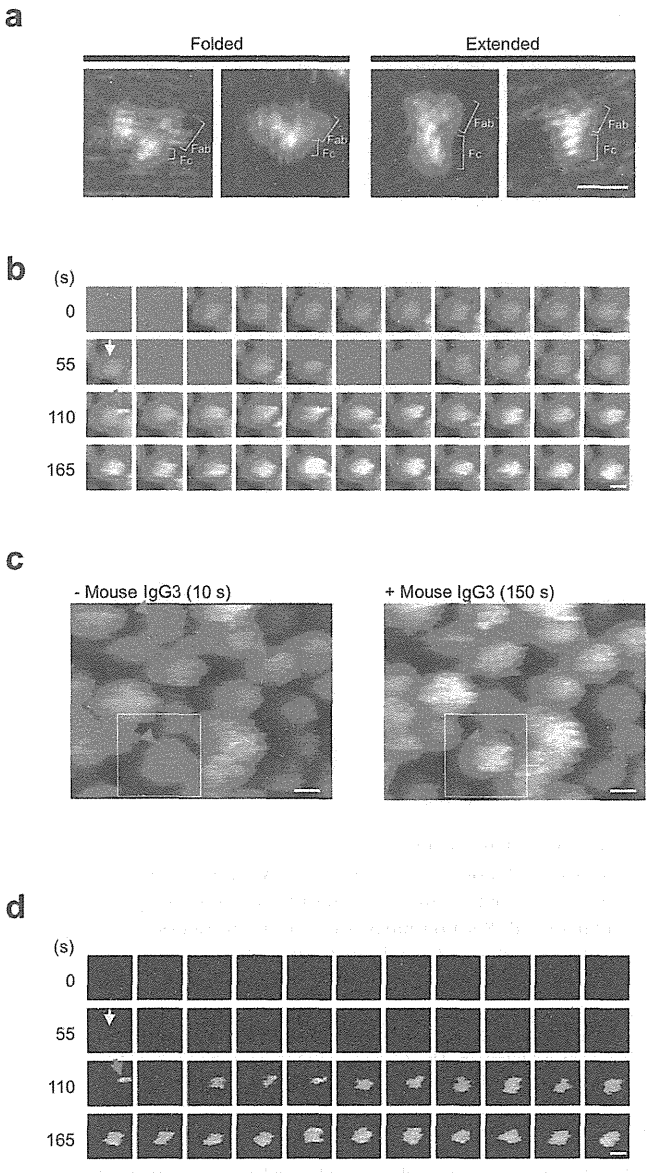

Figure 2 | HS-AFM analyses of mouse IgG3 and ZZ-BNC in solution. (a) HS-AFM images of mouse IgG3 molecules. Bar, 20 nm. (b) Video image of the movement of mouse IgG3 on ZZ-BNC (0.2 fps). Yellow arrow, the addition of mouse IgG3. Red arrow, first appearance of attachment. Times (s) after the start of observation are indicated in the left margin. Bar, 20 nm. (c) HS-AFM images of ZZ-BNCs on a gold surface without (10 s, left panel)/with (150 s, right panel) mouse IgG3. ZZ-BNC used for (b) is indicated by a white box. The locations where mouse IgG3 appeared are indicated by red arrowheads. Bars, 20 nm. (d) Binarized video image of the movement of mouse IgG3 on ZZ-BNC (0.2 fps). Yellow arrow, the addition of mouse IgG3. Red arrow, first appearance of mouse IgG3. Times (s) after the start of observation are indicated in the left margin. Bar, 20 nm.

(red arrowheads in Fig. 2c) changed from 14.4, 19.6 and 12.6 nm (left panel) to 24.7, 27.7 and 18.0 nm (right panel), respectively. Next, the portion of attachments on ZZ-BNC was extracted with PaintShop Pro software by setting the height of the ZZ-BNC surface (14.4 nm) as a threshold (Fig. 2d and Supplementary Movie 2). The attachment appeared on the surface of ZZ-BNC 55 s after the addition of IgG (110 s from the start, red arrows in Figs. 2b and d), suggesting that mouse IgG3s were captured by ZZ-BNCs and retained during the observation.

Analyses of the movement of mouse IgG3 on ZZ-BNC. The positions of the centre of mass of attachments were calculated from their projected areas using ImageJ software and were found to exhibit a two-dimensional Gaussian distribution (major axis, 25.6 nm; minor axis, 20.4 nm; Fig. 3a). Because the length between the centre of mass of mouse IgG3 and the tip of the Fc subunit was estimated to be 19.1 ± 4.0 nm (*see above*), the deflection angle of mouse IgG3 on ZZ-BNC was estimated to be 88.1 ± 20.5 degrees. These results demonstrate that mouse IgG3s were tightly bound onto ZZ-BNC through the Fc subunit with Fab subunits swinging outwardly (Fig. 3b). The average speed of movement of mouse IgG3 was estimated as 4.6 ± 3.0 nm (13.8 ± 9.0 degrees) per 5 s (Fig. 3c). The speed fluctuated from 0.24 to 15.6 nm (0.74 ± 0.14 to 49.7 ± 10.1 degrees) per 5 s (Fig. 3d). It has been reported that the diffusion coefficient of monomeric human IgG is $\sim 4 \times 10^{-7}$ cm^2 s^{-1}, implying that one IgG molecule can move spontaneously at 20 nm per 5 second[24]. These results indicate that IgG molecules on ZZ-BNC undergo rotational Brownian motion. ZZ-BNC acts as a scaffold for oriented-immobilization of IgGs, being expected to enhance the sensitivity and specificity of a wide range of immunosensors and immunoassays.

Discussion

The surface structure of BNC (recombinant yeast-derived HBsAg L protein particle) has been analyzed by conventional transmission electron microscopy (TEM) and AFM in air[8,9,25]. While rugged surface was suggested by TEM observation, no protrusion has so far been identified. Recently, the surface structure of native HBV virion has been analyzed by electron cryomicroscopy[17]. The envelope of HBV virion was decorated with 160–200 surface protrusions that are spaced ~6 nm apart. In this study, HS-AFM observation revealed for the first time that ZZ-BNC (a derivative of BNC) in solution displays 54 surface protrusions that are spaced 8.2 ± 1.7 nm apart. The small differences in space may be attributed to either the conditions for observation (air *versus* solution) or the mass of displayed molecules (~14-kDa pre-S region for HBV virion *versus* ~20-kDa ZZ domains for ZZ-BNC). Furthermore, during the biosynthesis of HBsAg particle in recombinant mammalian cells, nascent HBsAgs were shown to translocate across endoplasmic reticulum (ER) membrane along with the formation of intramolecular disulfide bonds, dimerize by forming intermolecular disulfide bonds, and then spontaneously assemble into particle structure without forming multimers[19]. But, while recombinant yeast-derived HBsAg L proteins (including HBsAg S and M proteins) form multimers by intermolecular disulfide bonds[8], it has not been determined if they form dimers or not prior to the formation of BNC. In this study, nascent ZZ-L proteins (a derivative of HBsAg L protein) translocated across yeast ER membrane were strongly suggested to dimerize firstly, assemble to particle structures, and then form multimers by intermolecular disulfide bonds. Therefore, it was considered that more oxidative conditions of protein biosynthesis in yeast cells[26] rather than mammalian cells[27] might contribute to the formation of multimeric HBsAg proteins in yeast cells[8].

In the development of biosensors, it is indispensable to decipher the direction, shape, and movement of sensing molecules on solid phase for improving sensitivity, specificity, and analyte-binding capacity. Conventionally, these molecules have been analyzed by electron microscopy (EM) and AFM[12–14]. While both methods allowed us to observe IgGs at single molecule level, the former could be operable only in air. However, they could neither achieve real-time observation of IgGs in solution nor distinguish Fc from Fab clearly. Exceptionally, Garcia *et al.* have succeeded in identifying the position of the Fc and Fab fragments in air by tapping-mode AFM[28,29]. The technical defects of these methods have forced us to evaluate the sensing molecules on solid phase by indirect methods (*i.e.*, functional analyses). For example, in case of immunosensors, the degree of

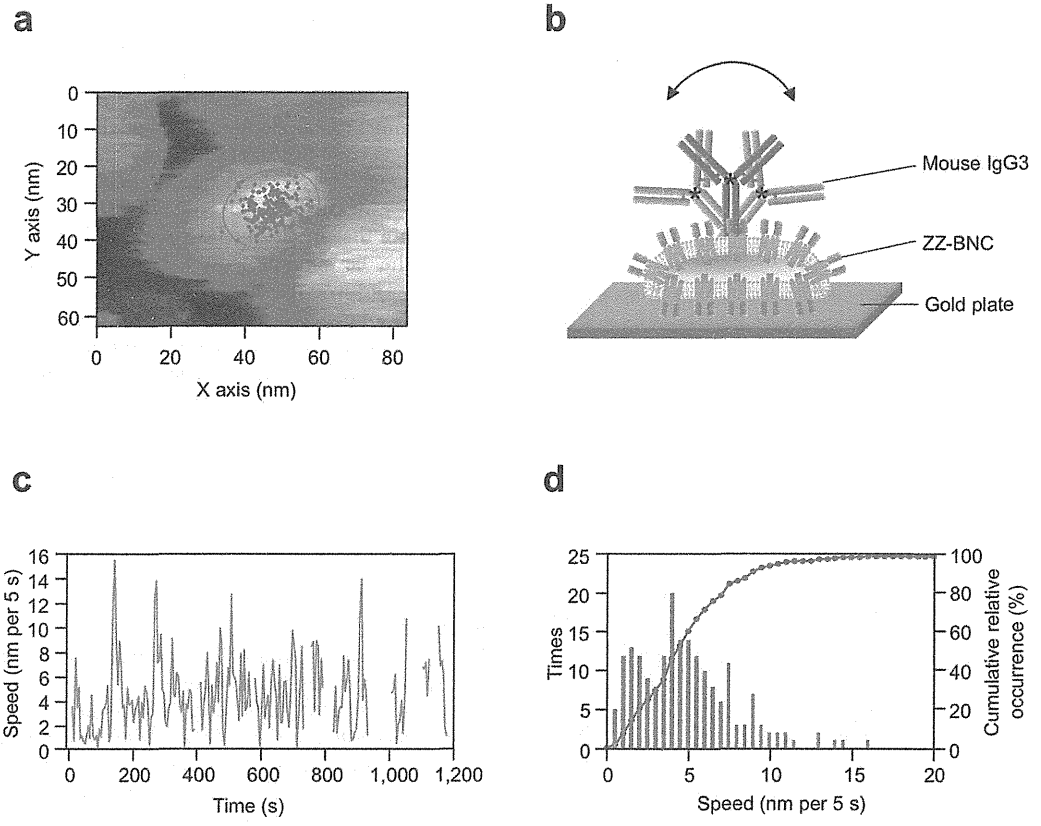

Figure 3 | Analyses of the movement of mouse IgG3 on ZZ-BNC. (a) Positions of the centre of mass of mouse IgG3 on ZZ-BNC are shown with blue dots (n = 210). The 99% confidence level is indicated by the red circle. (b) Postulated structure of mouse IgG3 on ZZ-BNC. Mouse IgG3 was tightly bound onto ZZ-BNC through the Fc subunit with Fab subunits swinging outwardly. Centres of mass of IgGs are indicated with black asterisks. (c) Relationship between speed (nm per 5 s) and time (s) for the movement of mouse IgG3 (centre of mass). (d) Relationship between occurrence and speed (nm per 5 s) of the movement of mouse IgG3 (centre of mass). Cumulative relative occurrence (%) of each speed is indicated with a blue line.

oriented immobilization of IgGs has been evaluated by the reactivity to antigens[30]. These indirect methods are indeed suitable for the optimization of biosensors, but it is equivocal to judge if sensing molecules exert their ability as much as possible. In this study, we could directly observe real-time movement of mouse IgG3s tethered onto ZZ-BNCs in solution by HS-AFM. It was therefore confirmed that ZZ-BNCs achieved oriented immobilization of IgGs, which has been hypothesized by functional analyses[9–11], by tethering Fc subunits in nearly close-packed arrangement and minimizing the steric hindrance of Fv regions for efficient antigen bindings. Since ZZ-BNCs are stable to heat, chemical, and mechanical stresses[9], ZZ-BNCs would be an ideal and practical scaffold for oriented immobilization of IgGs.

When observing the surface of biosensors by EM and AFM, it is essentially difficult to identify what molecules are adsorbed onto solid phase. For the molecular identification in EM, samples are usually pre-treated with labelling reagents (*e.g.*, gold particle-labelled antibodies). Worse yet, since conventional AFM can detect the ruggedness of sample surface only, it is nearly impossible to identify the molecules on the surface of mixed samples. On the contrary, HS-AFM can identify the molecules on the surface of solid phase by their movements without any modification. Taken together, HS-AFM might be worthwhile for the refinement of other biosensing molecules (*e.g.* ligands, receptors, aptamers, sugar chains, lectins) in various biosensors at the single molecule level.

Methods

ZZ-BNCs. ZZ-BNCs were overexpressed in *Saccharomyces cerevisiae* AH22R$^-$ cells carrying the ZZ-BNC-expression plasmid pGLD-ZZ50[7,8]. Following a previously described purification protocol for BNC[31], ZZ-BNCs were extracted from yeast cells by disruption with glass beads and purified using an AKTA™ liquid chromatography system (GE Healthcare, Amersham, UK) by affinity chromatography on porcine IgG, followed by gel filtration. The ZZ-BNCs were analyzed by 12.5% SDS-PAGE, followed by silver staining (Wako Chemicals, Osaka, Japan).

High-speed AFM. Topology images of ZZ-BNCs and mouse IgG3s (Sigma-Aldrich, St Louis, MO, USA) were obtained on a high-speed AFM system (Nano Live Vision, RIBM, Tokyo, Japan) using a silicon nitride cantilever (BL-AC10EGS, Olympus, Tokyo, Japan). To obtain static images, either ZZ-BNCs (50 μg ml^{-1}, 2 μl) or mouse IgG3s (1 μg ml^{-1}, 2 μl) were adsorbed on a mica surface (Ted Pella Inc., Redding, CA, USA), incubated for 10 min, washed with phosphate-buffered saline (PBS) three times, and then subjected to time-lapse imaging. To observe the real-time movement of IgGs on ZZ-BNC in solution, ZZ-BNCs (50 μg ml^{-1}, 2 μl) were adsorbed onto an atomically flat gold surface (Auro sheet (111) HS; Tanaka Kikinzoku Kogyo K.K., Tokyo, Japan), incubated for 10 min, washed with PBS three times, subjected to time-lapse imaging (0 s), and then mixed with mouse IgG3 (50 μg ml^{-1}, 4 μl) (55 s). Images (192 × 144 pixels) were obtained at a scan rate of 0.2 frames per second (fps) for 1,300 s. Images were analyzed by ImageJ 1.44o software (http://rsbweb.nih.gov/ij/) and PaintShop Pro software (COREL Corporation, Ontario, Canada). Semi-automated, single-particle reconstructions were performed using the EMAN software package, v1.9[16]. Ten particles were selected from 48 frames of the HS-AFM movies (total 761 frames) using the *boxer* program in the EMAN package.

1. Wink, T., van Zuilen, S. J., Bult, A. & van Bennkom, W. P. Self-assembled monolayers for biosensors. *Analyst* **122**, 43R–50R (1997).
2. Lu, B., Smyth, M. R. & O'Kennedy, R. Oriented immobilization of antibodies and its applications in immunoassays and immunosensors. *Analyst* **121**, 29R–32R (1996).
3. Gersten, D. M. & Marchalonis, J. J. A rapid, novel method for the solid-phase derivatization of IgG antibodies for immune-affinity chromatography. *J. Immunol. Methods.* **24**, 305–309 (1978).
4. Björck, L. & Kronvall, G. Purification and some properties of streptococcal protein G, a novel IgG-binding reagent. *J. Immunol.* **133**, 969–974 (1984).
5. O'Shannessy, D. J. & Quarles, R. H. Labeling of the oligosaccharide moieties of immunoglobulins. *J. Immunol. Methods* **99**, 153–161 (1987).

6. Prisyazhnoy, V. S., Fusek, M. & Alakhov, Y. Synthesis of high-capacity immunoaffinity sorbents with oriented immobilized immunoglobulins or their Fab' fragments for isolation of proteins. *J. Chromatogr.* **424**, 243–253 (1988).
7. Kurata, N. *et al.* Specific protein delivery to target cells by antibody-displaying bionanocapsules. *J. Biochem.* **144**, 701–707 (2008).
8. Kuroda, S., Otaka, S., Miyazaki, T., Nakao, M. & Fujisawa, Y. Hepatitis B virus envelope L protein particles. Synthesis and assembly in *Saccharomyces cerevisiae*, purification and characterization. *J. Biol. Chem.* **267**, 1953–1961 (1992).
9. Iijima, M. *et al.* Nanocapsules incorporating IgG Fc-binding domain derived from *Staphylococcus aureus* protein A for displaying IgGs on immunosensor chips. *Biomaterials* **32**, 1455–1464 (2011).
10. Iijima, M. *et al.* Bionanocapsule-based enzyme-antibody conjugates for enzyme-linked immunosorbent assay. *Anal. Biochem.* **396**, 257–261 (2010).
11. Iijima, M. *et al.* Fluorophore-labeled nanocapsules displaying IgG Fc-binding domains for the simultaneous detection of multiple antigens. *Biomaterials* **32**, 9011–9020 (2011).
12. Dutta, P., Sawoo, S., Ray, N., Bouloussa, O. & Sarkar, A. Engineering bioactive surfaces with Fischer carbene complex: protein A on self-assembled monolayer for antibody sensing. *Bioconjug. Chem.* **22**, 1202–1209 (2011).
13. Bendikov, T. A, Rabinkov, A., Karakouz, T., Vaskevich, A. & Rubinstein, I. Biological sensing and interface design in gold island film based localized plasmon transducers. *Anal Chem.* **80**, 7487–7498 (2008).
14. Lv, Z., Wang, J., Chen, G. & Deng, L. Imaging recognition events between human IgG and rat anti-human IgG by atomic force microscopy. *Int. J. Biol. Macromol.* **47**, 661–667 (2010).
15. Kodera, N., Yamamoto, D. & Ando, T. Video imaging of walking myosin V by high-speed atomic force microscopy. *Nature* **468**, 72–76 (2010).
16. Ludtke, S. J., Baldwin, P. R. & Chiu, W. EMAN: semiautomated software for high-resolution single-particle reconstructions. *J. Struct. Biol.* **128**, 82–97 (1999).
17. Dryden, K. A. *et al.* Native hepatitis B virions and capsids visualized by electron cryomicroscopy. *Mol. Cell* **22**, 843–850 (2006).
18. Eble, B. E., Lingappa, V. R. & Ganem, D. Hepatitis B surface antigen: an unusual secreted protein initially synthesized as a transmembrane polypeptide. *Mol. Cell. Biol.* **6**, 1454–1463 (1986).
19. Whunderlich, G. & Bruss, V. Characterization of early hepatitis B virus surface protein oligomers. *Arch. Virol.* **141**, 1191–1205 (1996).
20. Nagaoka, T. *et al.* Characterization of bio-nanocapsules as a transfer vector targeting human hepatocyte carcinoma by disulfide linkage modification. *J. Control. Release.* **118**, 348–356 (2007).
21. Palczewski, K. *et al.* Crystal structure of rhodopsin: a G protein-coupled receptor. *Science* **289**, 739–745 (2000).
22. Thomson, N. H. The substructure of immunoglobulin G resolved to 25 kDa using amplitude modulation AFM in air. *Ultramicroscopy* **105**, 103–110 (2005).
23. Thomson, N. H. Imaging the substructure of antibodies with tapping-mode AFM in air: the importance of a water layer on mica. *J. Microsc.* **217**, 193–199 (2005).
24. Jøssang, T., Feder, J. & Rosenqvist, E. Photon correlation spectroscopy of human IgG. *J. Protein Chemistry* **7**, 165–171, (1988).
25. kanno, T. *et al.* Size distribution measurement of vesicles by atomic force microscopy. *Anal. Biochem.* **309**, 196–199 (2002).
26. Frand, A. R. & Kaiser, C. A. Ero1p oxidized protein disulfide isomerise in a pathway for disulfide bond formation in the endoplasmic reticulum. *Mol. Cell* **4**, 469–477 (1999).
27. Jessop, C. E. & Bulleid, N. J. Glutathione directly reduces an oxidoreductase in the endoplasmic reticulum of mammalian cells. *J. Biol. Chem.* **279**, 55341–55347 (2004).
28. San Paulo, A. & García, R. High-resolution imaging of antibodies by tapping-mode atomic force microscopy: attractive and repulsive tip-sample interaction regimes. *Biophys. J.* **78**, 1599–1605 (2000).
29. Patil, S., Martinez, N. F., Lozano, J. R. & García, R. Force microscopy imaging of individual protein molecules with sub-pico Newton force sensitivity. *J. Mol. Recognit.* **20**, 516–523 (2007).
30. Song, H. Y., Zhou, X., Hobley, J. & Su, X. Comparative study of random and oriented antibody immobilization as measured by dual polarization interferometry and surface plasmon resonance spectroscopy. *Langmuir* **28**, 997–1004 (2012).
31. Jung, J. *et al.* Efficient and rapid purification of drug- and gene-carrying bio-nanocapsules, hepatitis B virus surface antigen L particles, from *Saccharomyces cerevisiae*. *Protein Expr. Purif.* **78**, 149–155 (2011).
32. Nilsson, B. *et al.* A synthetic IgG-binding domain based on staphylococcal protein A. *Protein Eng.* **1**, 107–113 (1987).

Acknowledgments

We thank Profs. K. Namba and T. Kato (Osaka University) for helpful advice and the Research Institute of Biomolecule Metrology Inc. for technical support. This work was supported in part by The Naito Foundation (to SK), the Canon Foundation (K09-00051, to SK), KAKENHI (Grant-in-Aid for Scientific Research (A) (21240052, to SK); Grant-in-Aid for Young Scientists (B) (23710143, to MI)), the Program for Promotion of Basic and Applied Researchers for Innovations in Bio-Oriented Industry (BRAIN) (to SK), and the Health Labour Sciences Research Grant from the Ministry of Health Labour and Welfare (to SK).

Author contributions

M.I. designed and performed the experiments, analyzed the data, and wrote the manuscript. M.S., N.Y. and T.N. gave helpful comments. S.K. designed and supervised the experiments, analyzed the data, and wrote the manuscript.

Additional information

Supplementary information accompanies this paper at http://www.nature.com/scientificreports

Competing financial interests: The authors declare no competing financial interests.

How to cite this article: Iijima, M., Somiya, M., Yoshimoto, N., Niimi, T. & Kuroda, S. Nano-visualization of oriented-immobilized IgGs on immunosensors by high-speed atomic force microscopy. *Sci. Rep.* **2**, 790; DOI:10.1038/srep00790 (2012).